

Contract No. F61775-00-WE028

FINAL REPORT

Advanced Guidance Law Design

Based on the Information-Set Concept

20 March 2001

REPORT DOCUMENTATION PAGE

1. REPORT DATE (DD-MM-YYYY) 22-03-2001	2. REPORT TYPE Final Report	3. DATES COVERED (FROM - TO) xx-xx-2001 to xx-xx-2001
4. TITLE AND SUBTITLE Advanced Guidance Law Design Based on the Information-Set Concept Unclassified		5a. CONTRACT NUMBER
		5b. GRANT NUMBER
		5c. PROGRAM ELEMENT NUMBER
6. AUTHOR(S) Rubinovich, Eugene Y. ;		5d. PROJECT NUMBER
		5e. TASK NUMBER
		5f. WORK UNIT NUMBER
7. PERFORMING ORGANIZATION NAME AND ADDRESS Institute of Control Sciences of Russian Academy of Sciences 65, Profsoyuznaya Str. Moscow , Russia 117806		8. PERFORMING ORGANIZATION REPORT NUMBER
9. SPONSORING/MONITORING AGENCY NAME AND ADDRESS ,		10. SPONSOR/MONITOR'S ACRONYM(S)
		11. SPONSOR/MONITOR'S REPORT NUMBER(S)
12. DISTRIBUTION/AVAILABILITY STATEMENT A PUBLIC RELEASE ,		

13. SUPPLEMENTARY NOTES
14. ABSTRACT This report results from a contract tasking Institute of Control Sciences of Russian Academy of Sciences as follows: Contractor will investigate development of new approaches to guidance algorithm design using the concepts of information set theory.
15. SUBJECT TERMS EOARD; Guidance

16. SECURITY CLASSIFICATION OF:			17. LIMITATION OF ABSTRACT Public Release	18. NUMBER OF PAGES 44	19a. NAME OF RESPONSIBLE PERSON Fenster, Lynn lfenster@dtic.mil
a. REPORT Unclassified	b. ABSTRACT Unclassified	c. THIS PAGE Unclassified			19b. TELEPHONE NUMBER International Area Code Area Code Telephone Number 703 767-9007 DSN 427-9007

REPORT DOCUMENTATION PAGE			Form Approved OMB No. 0704-0188	
Public reporting burden for this collection of information is estimated to average 1 hour per response, including the time for reviewing instructions, searching existing data sources, gathering and maintaining the data needed, and completing and reviewing the collection of information. Send comments regarding this burden estimate or any other aspect of this collection of information, including suggestions for reducing this burden to Washington Headquarters Services, Directorate for Information Operations and Reports, 1215 Jefferson Davis Highway, Suite 1204, Arlington, VA 22202-4302, and to the Office of Management and Budget, Paperwork Reduction Project (0704-0188), Washington, DC 20503.				
1. AGENCY USE ONLY (Leave blank)		2. REPORT DATE 22-March-2001		3. REPORT TYPE AND DATES COVERED Final Report
4. TITLE AND SUBTITLE Advanced Guidance Law Design Based on the Information-Set Concept			5. FUNDING NUMBERS F61775-00-WE028	
6. AUTHOR(S) Eugene Y Rubinovich				
7. PERFORMING ORGANIZATION NAME(S) AND ADDRESS(ES) Institute of Control Sciences of Russian Academy of Sciences 65, Profsoyuznaya Str. Moscow 117806 Russia			8. PERFORMING ORGANIZATION REPORT NUMBER N/A	
9. SPONSORING/MONITORING AGENCY NAME(S) AND ADDRESS(ES) EOARD PSC 802 BOX 14 FPO 09499-0200			10. SPONSORING/MONITORING AGENCY REPORT NUMBER SPC 00-4028	
11. SUPPLEMENTARY NOTES				
12a. DISTRIBUTION/AVAILABILITY STATEMENT Approved for public release; distribution is unlimited.			12b. DISTRIBUTION CODE A	
13. ABSTRACT (Maximum 200 words) This report results from a contract tasking Institute of Control Sciences of Russian Academy of Sciences as follows: Contractor will investigate development of new approaches to guidance algorithm design using the concepts of information set theory.				
14. SUBJECT TERMS EOARD, Guidance			15. NUMBER OF PAGES 43	
			16. PRICE CODE N/A	
17. SECURITY CLASSIFICATION OF REPORT UNCLASSIFIED	18. SECURITY CLASSIFICATION OF THIS PAGE UNCLASSIFIED	19. SECURITY CLASSIFICATION OF ABSTRACT UNCLASSIFIED	20. LIMITATION OF ABSTRACT UL	

NSN 7540-01-280-5500

Standard Form 298 (Rev. 2-89)
Prescribed by ANSI Std. Z39-18
298-102

Advanced Guidance Law Design Based on the Information-Set Concept

Eugene Rubinovich

Boris Miller

Dmitry Emel'yanov

Institute of Control Sciences, 65 Profsoyuznaya str., 117997, Moscow, Russia

Fax: (095) 420 2016

Abstract

A new approach to guidance algorithm design using the concept of the information sets (IS) is considered. As an example of such approach, the model of defense scenario against reentering ballistic missile is investigated. In this scenario, a maneuverable decelerating target is to be destroyed by a hit-to-kill interceptor using an IR array seeker and lateral impulse thrusters. The key element of the proposed approach is a description of the "interceptor-target" system state by means of IS. The numerical methods for fast transformations of the IS are developed.

Contents

1	Introduction	4
2	Problem statement	5
3	Information sets construction	7
4	Auxiliary impulse control problem	9
5	Solution of auxiliary control problem	11
6	The guidance algorithm against a maneuvering target based on the IS concept	14
6.1	Simple one-dimensional example	14
6.2	Problem of guidance to a maneuvering target	15
7	Monte Carlo test of the algorithm of guidance to a non-maneuvering target	17
7.1	A priori data	17
7.2	Evaluation of the guidance algorithm performance	19
7.3	Computational properties of the algorithm	19
7.4	Resume	27
8	Monte Carlo test of the algorithm of guidance to a maneuvering target	28
8.1	A priori data	28
8.2	Evaluation of the guidance algorithm performance	30
8.3	Computational properties of the algorithm	31
8.4	Results of the Monte Carlo simulation	31
8.5	Resume	32
9	Conclusion	33
10	Outlook	33

1 Introduction

The promising approach to the analysis of many problems of control with incomplete information has been developed in recent years. This approach is concerned with describing positions of the controlled system by so-called information set (IS), all points of which are compatible with the system's dynamics, control history, measurement model and observation history [1], [2]. In the framework of this approach the original control problem is reduced to a problem of control of the IS evolution. Usually, the aim of such control is to minimize some performance index as a function of information set.

This approach is especially suitable for problems of guidance with nonlinear (bearings/range, bearings-only) measurements corrupted by additive non-Gaussian noise distributed within given boundaries. It is well known that in such situations a Kalman-type estimator incorporated in the guidance loop usually fails for this measurement model, and overall guidance performance deteriorates significantly.

Using proposed IS-based approach, the three-dimensional problem of guidance with incomplete information is investigated. The impulse-controlled interceptor \mathbf{M} is guided to the maneuverable decelerating target \mathbf{T} . During the guidance the interceptor \mathbf{M} performs passive angle-type measurements corrupted by additive uniformly distributed noise. The aim of the guidance is a minimization of the relative distance to ensure target impact. An important feature of the problem is the fact that the interceptor's control impulses are orthogonal to its longitudinal axis, so the longitudinal component of the interceptor's motion is uncontrolled.

Similar problems were examined in works [3], [4] in the context of minimax filtration and the theory of differential games.

In the frame of this contract two different models of the target's relational motion are considered:

1. lateral acceleration in chosen coordinate system is constant but unknown;
2. lateral acceleration can change instantly remaining within given boundaries.

In both cases the longitudinal motion of interceptor and target is a deceleration caused by the drag forces. The drag coefficients are assumed to be known.

First, we consider the model No.1 with constant lateral acceleration caused by a drag force. More precisely the lateral acceleration is approximately constant. It changes much slower in the first model in contrast with jump-wise aerodynamical maneuvers in the second one. After formulation of a mathematical model of the guidance problem, we define the information sets for the considered dynamics. To facilitate numerical operations with the introduced IS we propose to use so-called Grid-Polygon Approximation of the IS.

As a criterion for the IS evolution control the miss averaged over IS is taken. The interceptor's control is chosen in the class of so-called "conditionally programmed controls", i.e. programmed controls which are updated after each measurement.

Recently, this approach has been applied to similar guidance problems in [5, 6] and very promising results have been obtained.

To update the control the auxiliary optimal impulse control problem is solved. In this problem a performance index has the meaning of expense of impulse control over time-to-go, and a terminal condition means zero average miss. The auxiliary problem is transformed to the quadratic mathematical programming problem which is solved using Kuhn-Tucker optimality conditions.

2 Problem statement

The guidance geometry is shown in Fig.1.

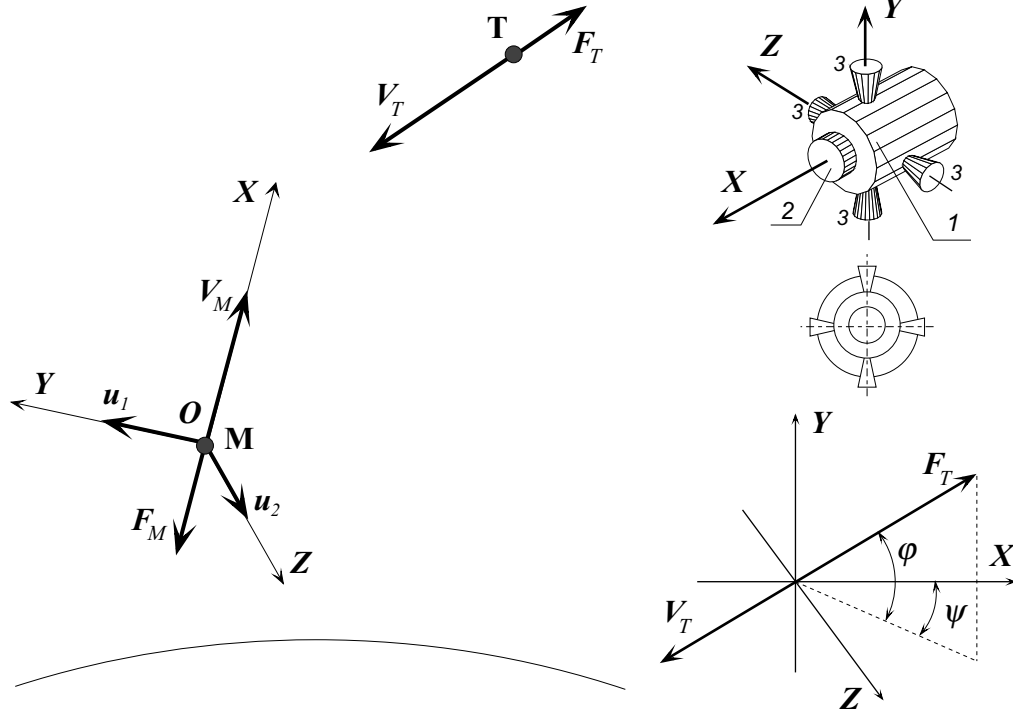


Figure 1: The guidance geometry. 1 – interceptor, 2 – IR array seeker, 3 – lateral impulse thrusters

It is assumed that the target \mathbf{T} moves with zero attack and sliding angles and the lift force can be neglected. Then the target's motion is a deceleration caused by the drag force:

$$V_T(t) = V_0 - \alpha_T \int_{t_0}^t V_T^2(s) ds, \quad \alpha_T = \frac{C_x S \rho}{2m_T}. \quad (1)$$

Here $V_T(t)$ – target's longitudinal velocity, m_T – target's mass, ρ – atmospheric density, S – target's frontal area, C_x – drag coefficient. The coefficient α_T is assumed

to be known. The relational motion of the interceptor \mathbf{M} and the target \mathbf{T} in the reference system \mathbf{OXYZ} fixed to the interceptor is described by the equations:

$$x(t) = x_0 - \int_{t_0}^t V_M(s) ds - \int_{t_0}^t k_x V_T(s) ds, \quad (2)$$

$$y(t) = y_0 - \int_{t_0}^t V_y(s) ds - \int_{t_0}^t k_y V_T(s) ds, \quad (3)$$

$$z(t) = z_0 - \int_{t_0}^t V_z(s) ds - \int_{t_0}^t k_z V_T(s) ds, \quad (4)$$

$$V_y(t) = \sum_{t_k \leq t} u_1(t_k), \quad V_z(t) = \sum_{t_k \leq t} u_2(t_k), \quad (5)$$

$$V_M(t) = W_0 - \alpha_M \int_{t_0}^t V_M^2(s) ds, \quad (6)$$

where t_0 – the initial instant of time, V_M, V_y, V_z – interceptor's velocities, $(u_1, u_2) = (u_1(t), u_2(t))$ – interceptor's impulse controls represented by a totality of impulses $u_{1k} = u_1(t_k), u_{2k} = u_2(t_k)$ which are applied at fixed instants $t_k = t_0 + k\Delta, k = 0, 1, \dots$; and Δ – given time interval. The constants k_x, k_y and k_z equal:

$$k_x = \cos \varphi \cos \psi, \quad k_y = \sin \varphi, \quad k_z = \cos \varphi \sin \psi.$$

The initial parameters x_0, y_0, z_0, V_0 and coefficients k_y, k_z are assumed to be unknown but restricted by the given inequalities.

During the guidance the interceptor performs measurements (ζ_{1k}, ζ_{2k}) described by the equations

$$\zeta_{1k} = \frac{y(t_k)}{x(t_k)} + \eta_{1k}, \quad \zeta_{2k} = \frac{z(t_k)}{x(t_k)} + \eta_{2k}, \quad k = 0, 1, \dots,$$

where η_{1k}, η_{2k} – uniformly distributed measurement noises:

$$|\eta_{1k}| \leq c, \quad |\eta_{2k}| \leq c,$$

c – given constant. The observation process and control process are terminated at an instant t_f , where

$$t_f = \inf\{t : x(t) < \varepsilon\}. \quad (7)$$

Here ε – given small distance, $\varepsilon > 0$. The physical meaning of the condition (7) is that target observations are impossible when the distance "interceptor-target" is lower than ε due to the large angular size of the target and overload of the seeker's IR receiver.

3 Information sets construction

By definition, the information set (IS) consists of all points of the phase space whose coordinates are compatible (in geometrical sense) with dynamics equations, measurement model and restrictions imposed on an initial state vector.

For the problem under consideration, the IS $I(t)$ is 6-dimensional one:

$$I(t) \subset \{x, V_T, y, z, k_y, k_z\},$$

assuming the coefficient k_x to be known.

Note that the dynamics equation described the motions along \mathbf{Y} and \mathbf{Z} axis as well as the corresponding measurement equations are functionally independent of each other. This fact lets us reduce the dimension of the IS and construct two 4-dim IS $I_y(t)$ and $I_z(t)$ instead of one 6-dim information set $I(t)$. Information sets $I_y(t)$ and $I_z(t)$ are constructed separately for subspaces $\{x, V_T, y, k_y\}$ and $\{x, V_T, z, k_z\}$.

In order to facilitate the numerical operations with IS, it is proposed to represent IS with the help of so-called Grid-Polygon Approximation (GPA) (Fig.2). For example, IS I_y is represented by a set of its sections for discrete values of x and V_T :

$$P_{ij}^y(t) \subset \{y, k_y\}, \quad i = 0, \dots, N_x - 1, \quad j = 0, \dots, N_V - 1,$$

$$P_{ij}^y(t) = I_y(t) \cap \{(x, V_T, y, k_y) : x = x_i(t), V_T = V_j(t)\},$$

where $(x_i(t), V_j(t))$ is a node of the 2-dim grid on the plane (x, V_T) . All sections $P_{ij}^y(t)$ are 2-dim polygons and each polygon corresponds to a certain node of the grid. The IS $I_z(t)$ is constructed in the same way.

During the guidance the evolution of an IS described by GPA consists of two processes:

- motion of the grid's nodes;
- evolution of the polygonal sections;

The evolution of each polygon after getting a measurement at some instant t_l is described by the equations:

$$P_{ij}^y(t_l) = P_{ij}^y(t_l-) \cap H_i^y, \quad P_{ij}^z(t_l) = P_{ij}^z(t_l-) \cap H_i^z,$$

where H_i^y, H_i^z are sets of uncertainty corresponding to the obtained measurement

$$H_i^y = \{(y, k_y) : \frac{y}{x_i} \in [\zeta_{1l} - c, \zeta_{1l} + c]\},$$

$$H_i^z = \{(z, k_z) : \frac{z}{x_i} \in [\zeta_{2l} - c, \zeta_{2l} + c]\}.$$

Here and later a sign "−" after time argument means left-side limit, for example

$$P_{ij}^y(t_l-) = \lim_{t \uparrow t_l} P_{ij}^y(t),$$

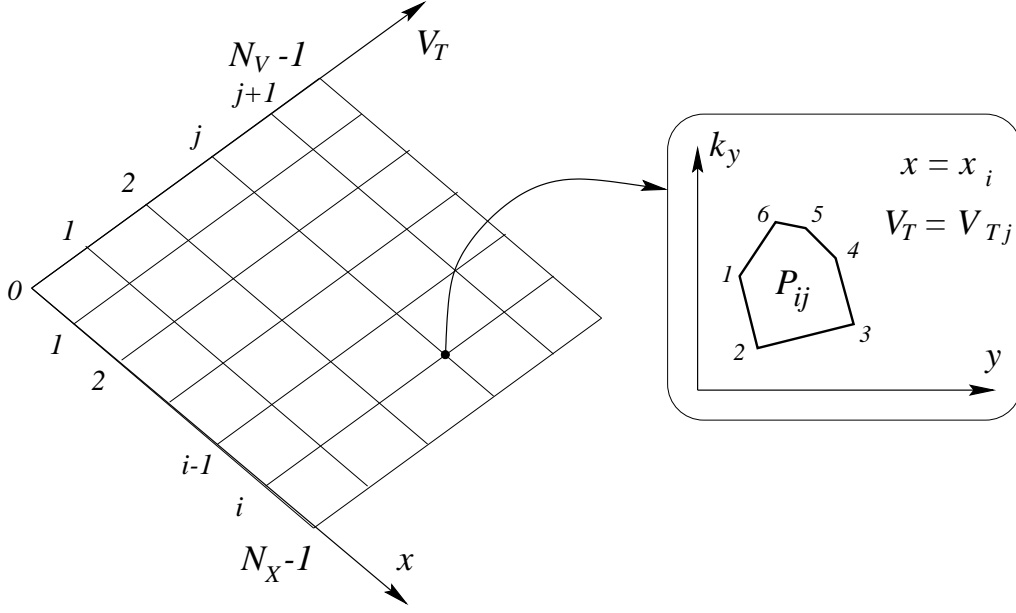


Figure 2: Grid-Polygon Approximation of an information set.

The evolution of the information sets on the interval $[t_l, t_{l+1}[$ is given by the equations

$$I_y(t_{l+1}-) = \mathcal{L}_y(u_{1l})I_y(t_l), \quad I_z(t_{l+1}-) = \mathcal{L}_z(u_{2l})I_z(t_l),$$

where $\mathcal{L}_y(\cdot)$ and $\mathcal{L}_z(\cdot)$ – one-step extrapolation operators, which can be found from (1)-(6) by integrating over $[t_l, t_l + \Delta]$ with some controls u_{1l} and u_{2l} :

$$V'_T = \frac{1}{\frac{1}{V_T} + \alpha_T \Delta}, \quad (8)$$

$$x' = x - \frac{1}{\alpha_M} \ln(1 + \alpha_M V_M(t_l) \Delta) - \frac{k_x}{\alpha_T} \ln(1 + \alpha_T V_T \Delta), \quad (9)$$

$$y' = y - \frac{k_y}{\alpha_T} \ln(1 + \alpha_T V_T \Delta) - u_{1l} \Delta - V_y(t_l) \Delta, \quad (10)$$

$$z' = z - \frac{k_z}{\alpha_T} \ln(1 + \alpha_T V_T \Delta) - u_{2l} \Delta - V_z(t_l) \Delta, \quad (11)$$

$$k'_y = k_y, \quad k'_z = k_z. \quad (12)$$

Here, the sign " ' " marks variables corresponding to the information sets $I_y(t_{l+1}-)$ and $I_z(t_{l+1}-)$, i.e.

$$(x', V'_T, y', k'_y) \in I_y(t_{l+1}-) \quad \text{and} \quad (x, V_T, y, k_y) \in I_y(t_l).$$

Analogously,

$$(x', V'_T, z', k'_z) \in I_z(t_{l+1}-) \quad \text{and} \quad (x, V_T, z, k_z) \in I_z(t_l).$$

The values $V_y(t_l)$ and $V_z(t_l)$ are calculated by (5).

In this terms we can define IS $\tilde{I}_y(t_n-)$ extrapolated to the end of the segment $[t_l, t_n[$:

$$\tilde{I}_y(t_n-) = \mathcal{L}_y(u_{1n-1}) \dots \mathcal{L}_y(u_{1l}) I_y(t_l). \quad (13)$$

The set $\tilde{I}_z^l(t_n-)$ is defined analogously. It is necessary to emphasize that extrapolated IS $\tilde{I}_y^l(t_n-)$ and $\tilde{I}_z^l(t_n-)$ are calculated without regard to future measurements, but with regard to future controls $\{u_{1l}, \dots, u_{1n-1}\}$ and $\{u_{2l}, \dots, u_{2n-1}\}$. Denote by $\tilde{I}_y^l(t_n)$ and $\tilde{I}_z^l(t_n)$ these sets with regard to terminal controls u_{1n} and u_{2n} .

4 Auxiliary impulse control problem

The aim of IS control is to minimize expected terminal miss $\mu = (\pi_y, \pi_z)$. This terminal miss can be approximated by the following equation:

$$\mu^2 = \pi_y^2 + \pi_z^2 = y^2(T) + z^2(T),$$

where the terminal moment T is defined by the condition

$$x(T) = 0.$$

Of course, the accurate values of the terminal miss as well as of the moment T are unknown. The idea is to introduce for each point A of the current IS a miss function $\Pi^l(A)$ – a vector-function with components $\Pi_y^l(A)$ and $\Pi_z^l(A)$. The component $\Pi_y^l(A)$ is equal to the terminal miss value (by Y axis) obtained on controlled motion of the system starting from the point A at instant t_l and averaged over extrapolated IS $\tilde{I}_y^l(T)$. The component $\Pi_z^l(A)$ is defined analogously. The function $\Pi^l(A)$ is taken as a measure of the real terminal miss.

Applying this idea to the GPA of the IS $I_y(t_0)$ and $I_z(t_0)$, let's calculate first the expected period of the motion τ_{ij}^0 for each node of the grid (and for each polygons). By integrating the corresponding dynamics equations, we obtain

$$V_T(t) = \frac{1}{\frac{1}{V_j} + \alpha_T(t - t_0)}, \quad V_M(t) = \frac{1}{\frac{1}{W_0} + \alpha_M(t - t_0)}$$

To integrate equations (2) and (3) we calculate an auxiliary integral

$$\int_{t_0}^t \frac{1}{\frac{1}{v} + \alpha(s - t_0)} ds = \frac{1}{\alpha} \ln(1 + \alpha v(t - t_0)) \quad (14)$$

By integrating (2) from the node $(x_i, V_j) = (x_i(t_0), V_j(t_0))$, in view of (14), we have

$$x(t) = x_i - \frac{1}{\alpha_M} \ln(1 + \alpha_M W_0(t - t_0)) - \frac{k_x}{\alpha_T} \ln(1 + \alpha_T V_j(t - t_0)). \quad (15)$$

It is clear that τ_{ij}^0 is a root of Eq. (15) when $x(t) = 0$, i.e.

$$x_i - \frac{1}{\alpha_M} \ln(1 + \alpha_M W_0 \tau_{ij}^0) - \frac{k_x}{\alpha_T} \ln(1 + \alpha_T V_j \tau_{ij}^0) = 0. \quad (16)$$

Assuming that the values τ_{ij}^0 are found by numerical solution of the Eq.(16) for all nodes, we can calculate the vector miss (π_y, π_z) for arbitrary instant $t = t_l$. Indeed, for the instant t_l

$$\tau_{ij}^l = \tau_{ij}^0 - (t_l - t_0). \quad (17)$$

It is assumed that if $\tau_{ij}^l < 0$ for some node this node will be excluded from the further calculation. Let (x_i, V_j, y, k_y) be a point of the IS $I_y(t_l)$. Then the miss π_y^l is calculated as follows:

$$\pi_y^l = y - \frac{k_y}{\alpha_T} \ln(1 + \alpha_T V_j \tau_{ij}^l) - \sum_{t_k \in [t_l, \theta^l]} u_{1k} (\tau_{ij}^l - (t_k - t_l)) - V_y(t_l) \tau_{ij}^l,$$

where θ^l is a lower-bound estimate of the time of control process termination defined by condition (7). By definition,

$$\theta^l = t_l + \Delta \left\lceil \frac{\tau_\varepsilon^l}{\Delta} \right\rceil, \quad (18)$$

where $[a]$ means an integer part of a , Δ is a time interval between the observations, and τ_ε^l is a root of the following equation

$$x_{\min}^l - \varepsilon - \frac{1}{\alpha_M} \ln(1 + \alpha_M V_M(t_l) \tau_\varepsilon^l) - \frac{k_x}{\alpha_T} \ln(1 + \alpha_T V_{\max}^l \tau_\varepsilon^l) = 0,$$

where

$$x_{\min}^l = \min_i x_i(t_l), \quad V_{\max}^l = \max_j V_j(t_l).$$

Then the expression for the averaged miss Π_y^l (analogously Π_z^l) takes the form

$$\Pi_y^l = \frac{1}{\tilde{Q}_y} \int_{\tilde{I}_y(\theta^l)} \pi_y^l d\tilde{x} d\tilde{V}_T d\tilde{y} d\tilde{k}_y, \quad (19)$$

where by a sign tilde we marked variables extrapolated to the moment θ^l . In particular $\tilde{I}_y(\theta^l)$ is the IS $I_y(t_l)$ extrapolated to the moment θ^l and \tilde{Q}_y is a volume of this extrapolated IS.

Now we can formulate an auxiliary control problem.

Problem 1. Let t_l be a current instant and $I_y(t_l)$ be information set after processing measurement ζ_{1l} . Let θ^l be predictable instant of control process termination given by (18). It is required to choose the impulse control $u_1(t_k) = u_{1k}$, $t_k \in [t_l, \theta^l]$ in order to minimize the performance index

$$\Phi_y^l(u) = \sum_{t_k \in [t_l, \theta^l]} u_{1k}^2 \quad (20)$$

and satisfy the terminal condition

$$\Pi_y^l = 0. \quad (21)$$

Problem 2 for control process $u_2(t_k) = u_{2k}$ is formulated analogously.

5 Solution of auxiliary control problem

It follows from (8)-(12) that the information set extrapolation (13) can be described by the following equations

$$\begin{aligned}\tilde{V}_T &= \frac{1}{\frac{1}{V_T} + \alpha_T \tau^l}, \\ \tilde{x} &= x - \frac{1}{\alpha_M} \ln(1 + \alpha_M V_M(t_l) \tau^l) - \frac{k_x}{\alpha_T} \ln(1 + \alpha_T V_T \tau^l), \\ \tilde{y} &= y - \frac{k_y}{\alpha_T} \ln(1 + \alpha_T V_T \tau^l) - \sum_{t_k \in [t_l, \theta^l]} u_{1k}(\tau^l - (t_k - t_l)) - V_y(t_l) \tau^l, \\ \tilde{k}_y &= k_y,\end{aligned}$$

where

$$(x, V_T, y, k_y) \in I_y(t_l), \quad (\tilde{x}, \tilde{V}_T, \tilde{y}, \tilde{k}_y) \in \tilde{I}_y(\theta^l).$$

Due to the introduced GPA, $x = x_i$ and $V_T = V_j$ for some node with number (i, j) , so τ^l equals to τ_{ij}^l from Eq. (17). These formulas define a change of variables in the integral (19). Jacobian of this exchanging is equal to

$$D_l = (1 + \alpha_T V_T \tau^l)^{-2}.$$

In this terms condition (21) takes the form

$$\begin{aligned}& \int_{I_y(t_l)} \left[y - \frac{k_y}{\alpha_T} \ln(1 + \alpha_T V_j \tau_{ij}^l) - V_y(t_l) \tau_{ij}^l - \right. \\ & \left. - \sum_{t_k \in [t_l, \theta^l]} u_{1k}(\tau_{ij}^l - (t_k - t_l)) \right] (1 + \alpha_T V_j \tau_{ij}^l)^{-2} dx dV_T dy dk_y = 0.\end{aligned}\quad (22)$$

Here, the integral over polygons can be calculated using Green's formula, the other two integrations (over dx and dV_T) can be made using grid approximation and Euler's formula.

To do this we calculate two auxiliary double integrals J_m^1 and J_m^2 over two-dimensional polygon σ_m , which defined by a set of its vertex $\{\xi_p, \eta_p\}$, $p = 1, \dots, m$. These integrals have the forms

$$J_m^1 = \int_{\sigma_m} \int_{\sigma_m} (\xi - \eta) d\xi d\eta, \quad J_m^2 = \int_{\sigma_m} \int_{\sigma_m} C d\xi d\eta, \quad C = \text{const.} \quad (23)$$

We have by Green's formula

$$J_m^1 = \int_{\sigma_m} \int_{\sigma_m} (\xi - \eta) d\xi d\eta = \int_{\Gamma_m} \xi \eta (d\xi + d\eta),$$

where Γ_m is a boundary of σ_m . The last integral is a sum of m integrals $J_m^1(p)$

$$J_m^1 = \sum_{p=1}^m J_m^1(p) = \sum_{p=1}^m \int_{\gamma_p} \xi \eta (d\xi + d\eta), \quad (24)$$

where each $J_m^1(p)$ is an integral over a segment γ_p with ends $\{\xi_p, \eta_p\}$ and $\{\xi_{p+1}, \eta_{p+1}\}$, $p = 1, \dots, m$. It is assumed that $\{\xi_{m+1}, \eta_{m+1}\} = \{\xi_1, \eta_1\}$. A segment γ_p admits a parametric description

$$\xi = \lambda(\xi_{p+1} - \xi_p) + \xi_p, \quad \eta = \lambda(\eta_{p+1} - \eta_p) + \eta_p, \quad \lambda \in [0, 1]. \quad (25)$$

Denoting $\Delta_{\xi p} = \xi_{p+1} - \xi_p$ and $\Delta_{\eta p} = \eta_{p+1} - \eta_p$, we get with the help of (25)

$$\begin{aligned} J_m^1(p) &= \int_{\gamma_p} \xi \eta (d\xi + d\eta) = \int_0^1 (\lambda \Delta_{\xi p} + \xi_p)(\lambda \Delta_{\eta p} + \eta_p)(\Delta_{\xi p} + \Delta_{\eta p}) d\lambda = \\ &= (\Delta_{\xi p} + \Delta_{\eta p}) \left[\xi_p \eta_p + \frac{\Delta_{\xi p} \eta_p + \Delta_{\eta p} \xi_p}{2} + \frac{\Delta_{\xi p} \Delta_{\eta p}}{3} \right]. \end{aligned} \quad (26)$$

Analogously, for the integral J_m^2 we have by Green's formula

$$J_m^2 = \int_{\sigma_m} C d\xi d\eta = \frac{C}{2} \int_{\Gamma_m} (\xi d\eta - \eta d\xi) = \sum_{p=1}^m J_m^2(p), \quad (27)$$

where

$$J_m^2(p) = \frac{C}{2} \int_{\gamma_p} (\xi d\eta - \eta d\xi) = \frac{C}{2} (\xi_p \Delta_{\eta p} - \eta_p \Delta_{\xi p}). \quad (28)$$

Now we calculate the integral (22). For this purpose we introduce the next notations:

$$a_{ij}^l(k) = \frac{\tau_{ij}^l - (t_k - t_l)}{(1 + \alpha_T V_j \tau_{ij}^l)^2},$$

$$b_{ij}^l = \frac{1}{\alpha_T} \ln(1 + \alpha_T V_j \tau_{ij}^l),$$

$$f_{ij}^l = \int_{P_{i,j}^y(t_l)} \int (y - k_y b_{ij}^l) \frac{1}{(1 + \alpha_T V_j \tau_{ij}^l)^2} dy dk_y,$$

$$h_{ij}^l = \int_{P_{i,j}^y(t_l)} \int V_y(t_l) \tau_{ij}^l \frac{1}{(1 + \alpha_T V_j \tau_{ij}^l)^2} dy dk_y,$$

where $P_{i,j}^y(t_l)$ is a polygon with vertices $\{y_p, k_{yp}\}$, $p = 1, \dots, m$, in the plane (y, k_y) corresponds to the grid node with number (i, j) (Fig.2).

Under fixed l, i, j we put

$$\xi = y \quad \text{and} \quad \eta = k_y b_{ij}^l.$$

Then a polygon $P_{i,j}^y(t_l)$ transforms to a polygon σ_m with vertices (ξ_p, η_p) where $\xi_p = y_p$ and $\eta_p = k_{yp} b_{ij}^l$, $p = 1, \dots, m$. In these notations

$$f_{ij}^l = \frac{1}{b_{ij}^l (1 + \alpha_T V_j \tau_{ij}^l)^2} J_m^1, \quad h_{ij}^l = \frac{V_y(t_l) \tau_{ij}^l}{(1 + \alpha_T V_j \tau_{ij}^l)^2} J_m^2 \quad (29)$$

where J_m^1 from (23) and it is calculated by formulas (24), (26); J_m^2 from (27) with constant $C = 1$.

Next, denote

$$g_{ij}^l(k) = \int \int_{P_{i,j}^y(t_l)} a_{ij}^l(k) dy dk_y = J_m^2,$$

where J_m^2 from (27) with constant $C = a_{ij}^l(k)$ and parameters $\xi_p = y_p$, $\eta_p = k_{yp}$. The value of this integral is calculated by (27) and (28).

As already mentioned above, we calculate the integral (22) by the variables x and V_T with the help of grid approximation and Euler's formula. This gives in view of introduced notations

$$F^l - \sum_{t_k \in [t_l, \theta^l]} u_{1k} G^l(k) = 0, \quad (30)$$

where

$$F^l = \sum_{i,j} (F_{ij}^l + F_{i+1j}^l + F_{ij+1}^l + F_{i+1j+1}^l), \quad F_{ij}^l = f_{ij}^l - h_{ij}^l,$$

$$G^l(k) = \sum_{i,j} (g_{ij}^l(k) + g_{i+1j}^l(k) + g_{ij+1}^l(k) + g_{i+1j+1}^l(k)).$$

Thus, we get a quadratic programming problem with the payoff function (20) and linear condition (30). To solve this problem, let's introduce the following Lagrangian function

$$L(u, \lambda) = \sum_{t_k \in [t_l, \theta^l]} u_{1k}^2 + \lambda \left(F^l - \sum_{t_k \in [t_l, \theta^l]} u_{1k} G^l(k) \right),$$

where $\lambda \geq 0$ is a Lagrange multiplier. It follows from Kuhn-Tucker theorem that the optimality condition for the control is

$$\frac{\partial L(u, \lambda)}{\partial u_{1k}} = 0, \quad k : t_k \in [t_l, \theta^l]. \quad (31)$$

From (31) and (30) we obtain the optimal control u_{1k}^* and parameter λ :

$$u_{1k}^* = \frac{G^l(k)F^l}{S^l}, \quad \lambda = \frac{2F^l}{S^l},$$

where

$$S^l = \sum_{t_k \in [t_l, \theta^l]} [G^l(k)]^2.$$

The optimal control impulse at instant t_l is given as

$$u_{1l}^* = \frac{G^l(l)F^l}{S^l}.$$

6 The guidance algorithm against a maneuvering target based on the IS concept

So far we considered only case of target's motion without any maneuvers. In this section, we will consider a maneuvering decelerating target lateral acceleration which can change instantly remaining within given boundaries. We will propose an approach to the treatment of possible target's maneuvers in the framework of the information-set concept.

6.1 Simple one-dimensional example

Let's consider one-dimensional motion with model

$$x(t) = x_0 + a(t),$$

where x_0 – an initial position, $a(\cdot)$ – a term describing possible target's maneuver:

$$|a(t)| \leq A_m, \quad t > t_0.$$

The initial position x_0 is unknown but assumed to belong to given interval I_0 which defines an initial IS. The model of measurements is very simple:

$$\zeta_i = x(t_i) + \eta_i,$$

where t_i are discrete instants of time, $t_i = t_0 + i\Delta$, η_i is a measurement noise assumed to be bound by the following inequality

$$|\eta_i| \leq c.$$

After each measurement the information set I_i^- transforms as follows

$$I_i = I_i^- \cap \{x : x \in [\zeta_i - c, \zeta_i + c]\}$$

The proposed treatment of possible target's maneuver is illustrated by Fig.3.

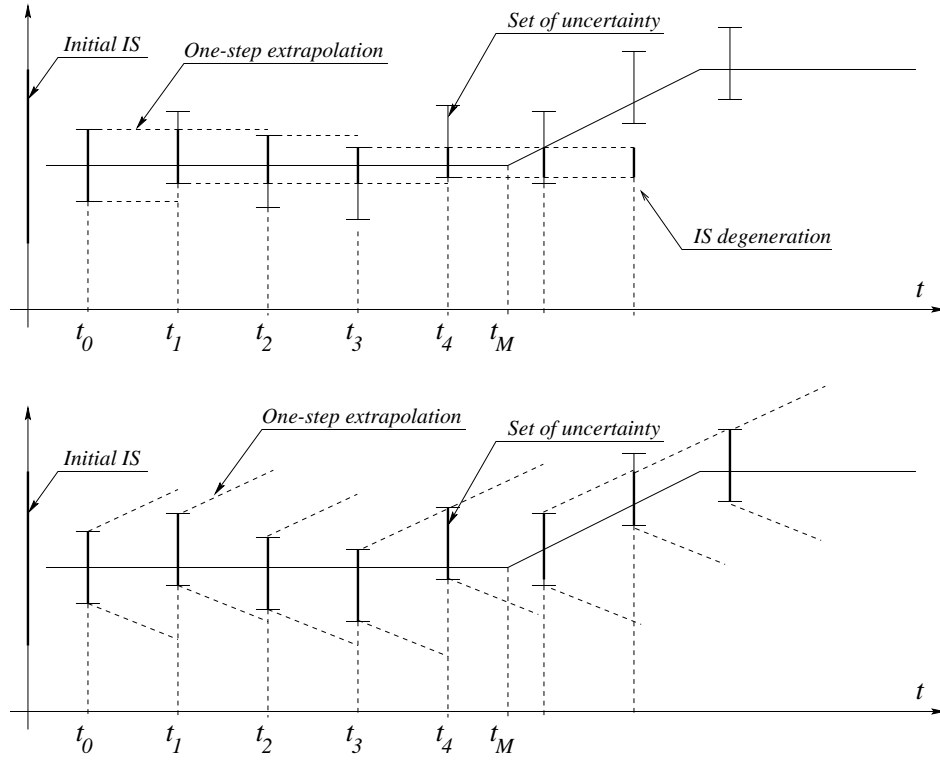


Figure 3: The behaviour of one-dimensional IS during a target's maneuver and proposed approach for its treatment.

The basic idea is to artificially increase size of the IS during one-step extrapolation between two neighboring measurements in order to prevent possible IS degeneration due to the maneuver. In our simple example, corresponding equation of one-step extrapolation has a form

$$I_{i+1}^- = [I_a - A_m \Delta, I_b + A_m \Delta],$$

where I_b and I_a are upper and lower ends of the IS I_i , respectively. Actually, this equation means that IS is to be inflated with maximal possible speed (A_m) on the intervals between measurements.

Let's apply this approach to the guidance problems considered in previous sections taking possible target's maneuvers into account.

6.2 Problem of guidance to a maneuvering target

The statement of guidance problem which we will consider is almost the same as in section 2 except for modified equations of "target-interceptor" motion.

In order to describe target's \mathbf{T} maneuvers it is assumed that the target can slightly change attack and sliding angles trying to avoid collision with the interceptor. Mathematically it may be formalized in the next form. Suppose that in

equations (3),(4) of "target-interceptor" motion

$$k_y(t) = \sin \varphi + \int_{t_0}^t a_y(s) ds, \quad (32)$$

$$k_z(t) = \cos \varphi \sin \psi + \int_{t_0}^t a_z(s) ds. \quad (33)$$

Terms $a_y(t)$, $a_z(t)$ account for possible target's maneuvers. The only information on these functions is that they are bounded by given inequalities

$$|a_y(t)| \leq A_y, \quad |a_z(t)| \leq A_z. \quad (34)$$

All the IS have the same construction as above, but their evolution on the interval $[t_l, t_{l+1}]$ is given by the equations

$$I_y(t_{l+1}-) = \mathcal{M}_y \mathcal{L}_y(u_{1l}) I_y(t_l),$$

$$I_z(t_{l+1}-) = \mathcal{M}_z \mathcal{L}_z(u_{2l}) I_z(t_l),$$

where $\mathcal{L}_y(\cdot)$ and $\mathcal{L}_z(\cdot)$ – one-step extrapolation operators, which can be found as above from (8)-(12), assuming that there is no target's maneuver in $[t_l, t_l + \Delta]$. Operators \mathcal{M}_y , \mathcal{M}_z perform linear transformation of the GPA's polygons in order to take target's maneuvers into account. As follows from the model of maneuver (32)–(34), each point (y, k_y) of a polygon is transformed into an interval $[(y^-, k_y^-), (y^+, k_y^+)]$ due to the possible maneuver:

$$\begin{aligned} y^- &= y - A_y L(V_T), & k_y^- &= k_y - A_y \Delta, \\ y^+ &= y + A_y L(V_T), & k_y^+ &= k_y + A_y \Delta, \end{aligned} \quad (35)$$

where the function $L(\cdot)$ can be obtained by integrating equation (3):

$$L(V_T) = \frac{\Delta}{\alpha_T} - \frac{1}{\alpha_T^2 V_T} \ln(1 + \alpha_T V_T \Delta).$$

Geometrically, such transformation is nothing but stretching of the GPA's polygons along a straight line with slope $L(V_T)/\Delta$ as shown in Fig.4. The extrapolated IS is calculated in the same way as for non-maneuvering target, i.e. regardless to future maneuvers of the target (see Eq. (13)). It means that we can use the same statement of the auxiliary impulse control problem for both maneuvering and non-maneuvering targets. Of course, the solution of the problem will be also the same.

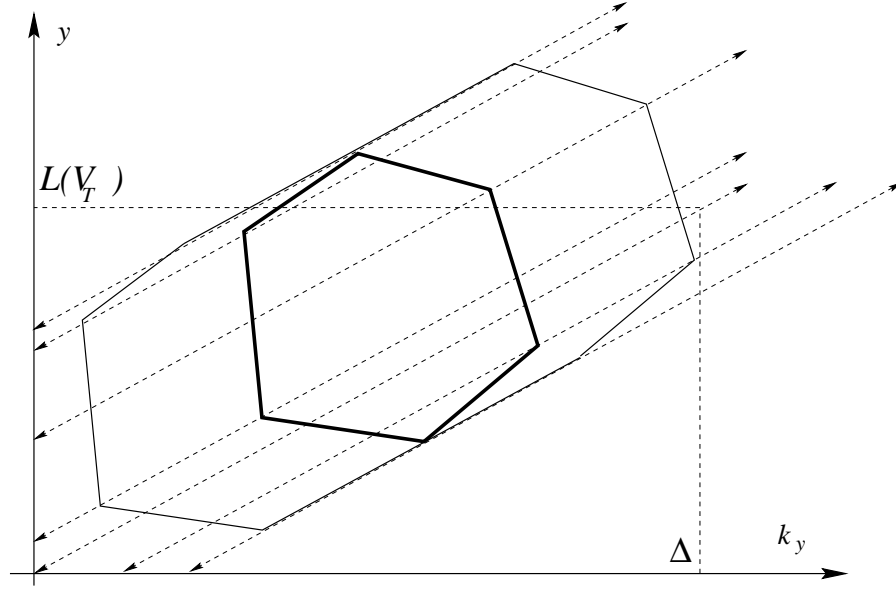


Figure 4: Transformation of the GPA's polygons.

7 Monte Carlo test of the algorithm of guidance to a non-maneuvering target

In this section, we present and discuss results of Monte Carlo tests which have been conducted for the algorithm of guidance to a non-maneuvering decelerating target. These results regarding to accuracy of guidance and expense of controlling impulses will be compared with the optimal solution of guidance problem with complete information.

Also we will consider aspects of the algorithm's program implementation and its computational properties, in particular, required computing time and numerical stability of the algorithm.

7.1 A priori data

The flow chart of the guidance process simulation in the case of constant lateral acceleration is shown in Fig.5.

The algorithm was implemented in C program module and tested on PC Pentium III 500 MHz.

The algorithm was tested on a model with parameters from Table.1.

The GPA consisted of $51 \times 51 = 2551$ nodes:

$$x_i = x_0 + i\Delta_x, \quad V_{Tj} = V_0 + j\Delta_V, \quad i, j = 0, \dots, 50,$$

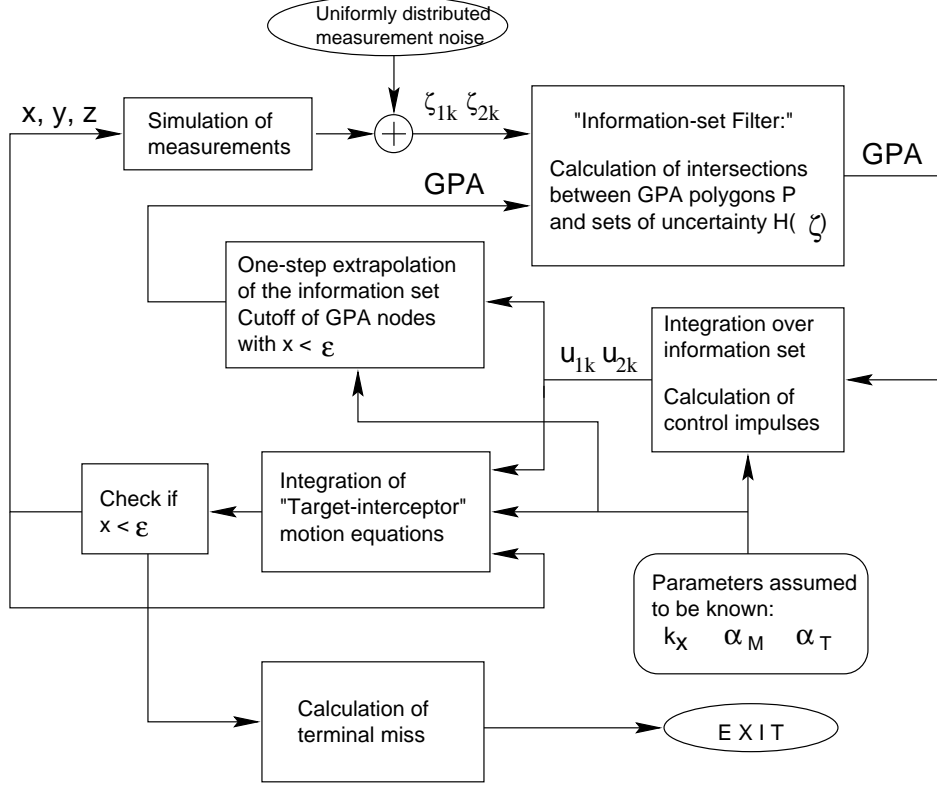


Figure 5: Simulation of the guidance process with constant lateral acceleration.

where

$$x_0 = 65000 \text{ m}, \quad \Delta_x = 200 \text{ m}, \quad V_0 = 4000 \text{ m/s}, \quad \Delta_V = 200 \text{ m/s}$$

The initial GPA polygons have been assumed to be rectangles defined by the following inequalities

$$\begin{aligned} y_0^* + \delta y \eta_y - \Delta_y &\leq y \leq y_0^* + \delta y \eta_y + \Delta_y, \\ z_0^* + \delta z \eta_z - \Delta_z &\leq z \leq z_0^* + \delta z \eta_z + \Delta_z, \\ \sin(\varphi - \Delta_\varphi) &\leq k_y \leq \sin(\varphi + \Delta_\varphi), \\ \cos(\varphi + \Delta_\varphi) \sin(\varphi - \Delta_\varphi) &\leq k_z \leq \cos(\varphi - \Delta_\varphi) \sin(\varphi + \Delta_\varphi), \end{aligned}$$

Parameter	Value	Parameter	Value
V_M	3000 m/s	α_M	$1.5 \cdot 10^{-5}$
V_T	4750 m/s	α_T	$2.0 \cdot 10^{-5}$
Δ	0.1 s	φ	-20 grad.
ψ	20 grad		

Table 1: Parameters used in the MC test.

Test number	c_y , rad	c_z , rad	Number of MC runs
1	0.001	0.001	1000
2	0.002	0.002	1000
3	0.003	0.003	1000

Table 2: Values of c_y , c_z parameters.

where y_0^* , z_0^* are initial positions which provide zero terminal miss on free (i.e. with zero controls) motion of the "target-interceptor" system, η_y , η_z – random values uniformly distributed over $[-1, 1]$ interval. The other parameters are the following

$$\begin{aligned} \delta y = 100 \text{ m}, \quad \delta z = 100 \text{ m}, \quad \Delta_y = 3000 \text{ m}, \quad \Delta_z = 3000 \text{ m}, \\ \Delta_\varphi = 5.0 \text{ grad}, \quad \Delta_\psi = 5.0 \text{ grad} \end{aligned}$$

The MC tests have been conducted for three different values of restrictions imposed on measurement errors represented in Table.2.

7.2 Evaluation of the guidance algorithm performance

To estimate performance of the guidance algorithm, the following values have been calculated after each MC run:

1. Terminal misses along **Y** and **Z** axis M_y , M_z .
2. Consumption of control impulses, R_y and R_z

$$R_y = \sum_{t_k < t_f} |u_{1k}|, \quad R_z = \sum_{t_k < t_f} |u_{2k}|,$$

where t_f is the instant of guidance process termination.

The corresponding distributions are shown in Fig.6 and Fig.7. Filled histograms in these figures show results for the optimal solution of guidance problem with exact information. Term "exact information" means that the initial parameters of the target's motion are taken from Monte Carlo truth. After that the deterministic problem of optimal control is solved. In this problem, the performance index is a minimization of control expenses while terminal conditions provide zero terminal miss.

7.3 Computational properties of the algorithm

In order to understand the computational properties of the proposed algorithm we have investigated

- Possibility of GPA degeneration when it prematurely collapses and there is no non-empty nodes at the end of the guidance.
- Convergence of GPA to the true values of x_0 and V_T parameters. In case of convergence all non-empty nodes of GPA should be located around point corresponding to the true values of x_0 and V_T .
- Computational speed of the algorithm and timing of different parts of the algorithmic procedure.

The histograms for the mean computing time and number of non-empty GPA nodes at the end of the guidance are presented in Fig.8 – 10.

One can see that zero bin of the histograms for the final number of GPA nodes is empty. It means that during all 3000 (3x1000) MC runs there were no cases of premature collapse of GPA regardless to the measurement accuracy.

The mean computing time and partial timing are summarized in Table.3.

Values of c_y, c_z , rad	0.001	0.002	0.003
Total mean time, s	4.06	4.76	5.26
Information set filter, s	1.19	1.33	1.43
Calculation of control, s	2.09	2.46	2.76
One-step GPA extrapolation, s	0.75	0.94	1.04

Table 3: MC test results on computational speed of the algorithm

The correct convergence of the GPA is illustrated by Fig.11 – 13. On these plots, the average GPA profiles are shown for different instants of time. By definition, the GPA profile is a two-dimensional distribution calculated as follows

$$\mathcal{P}_{ij}(t) = \frac{\sum_{k=0}^{N_{runs}} E_k(i, j, t)}{N_{runs}},$$

where N_{runs} – the number of MC runs taken for averaging, $E_k(i, j, t)$ equals to 1 if GPA node (i, j) at instant t is non-empty during MC run number k , and equals to 0 if this node is empty. The true values of x_0 , V_T parameters are marked by haircrosses.

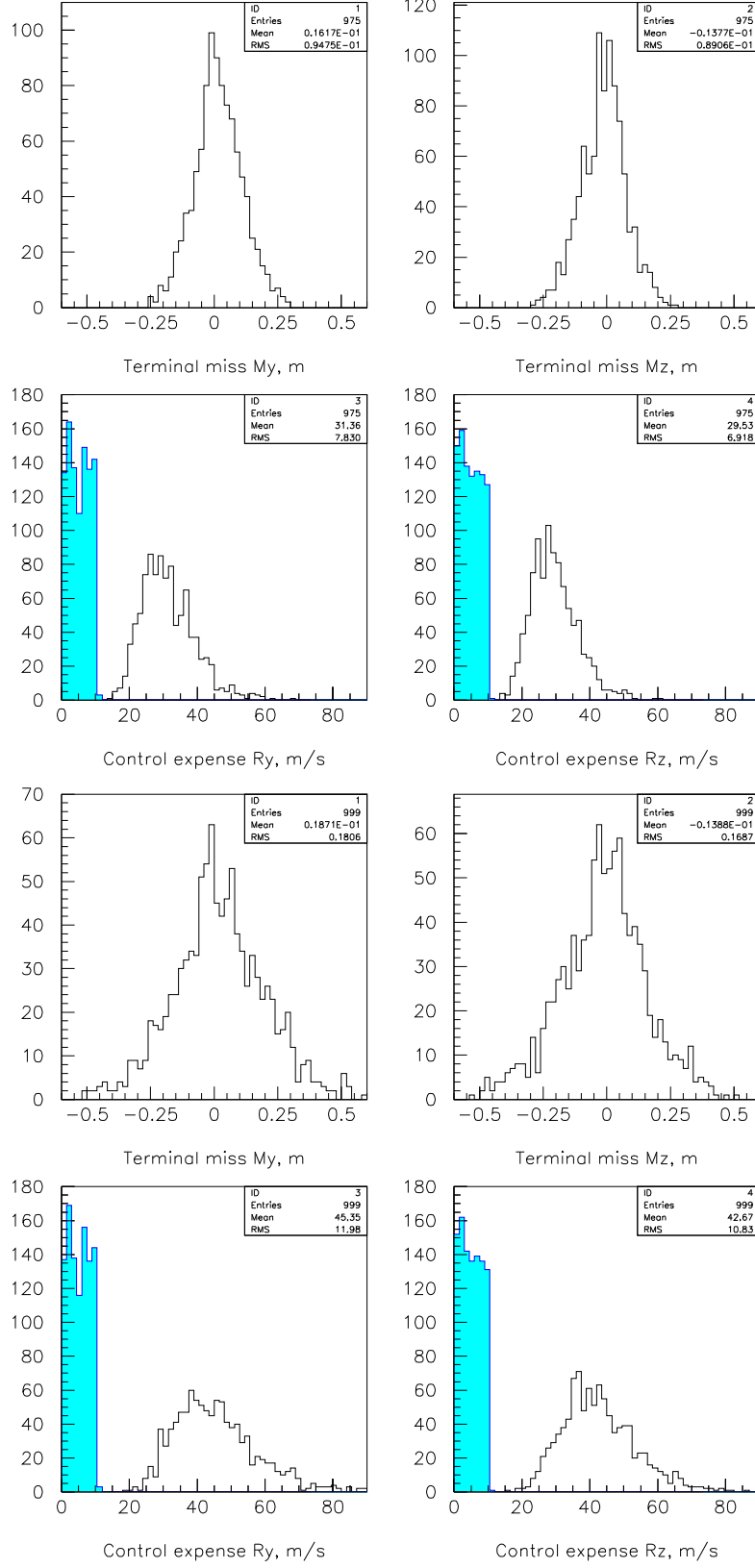


Figure 6: MC test results for $c_y = c_z = 0.001$ rad (upper two plots) and $c_y = c_z = 0.002$ rad.

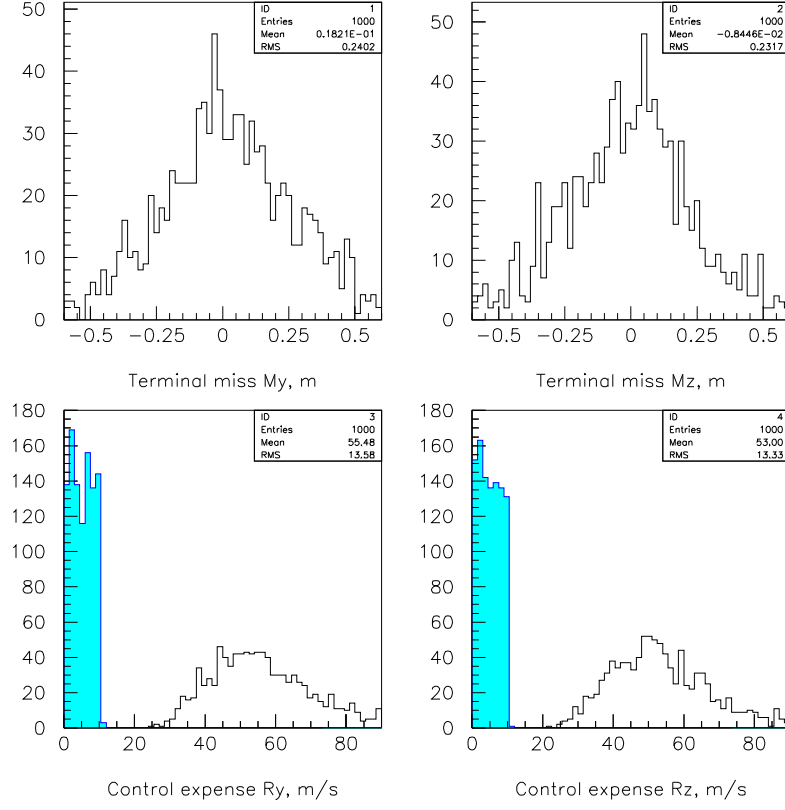


Figure 7: MC test results for $c_y = c_z = 0.003$ rad.

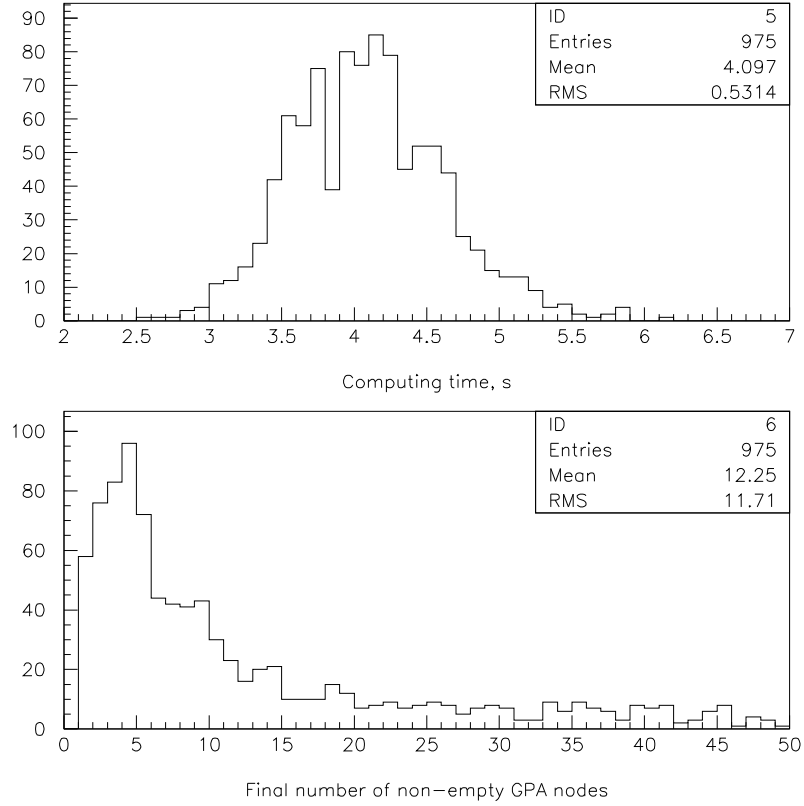


Figure 8: MC test results for $c_y = c_z = 0.001$ rad.

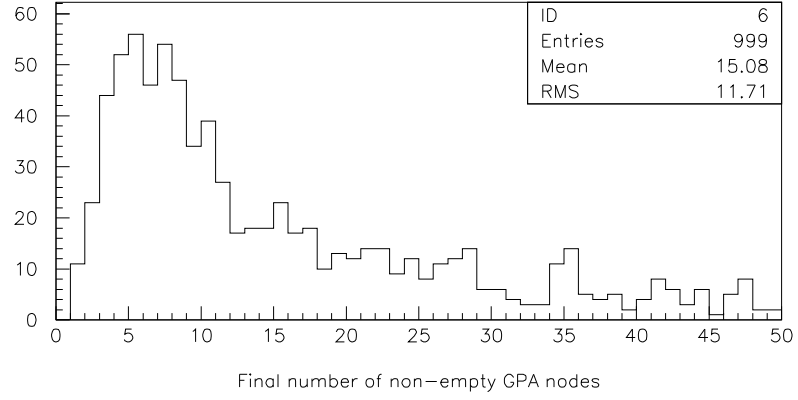
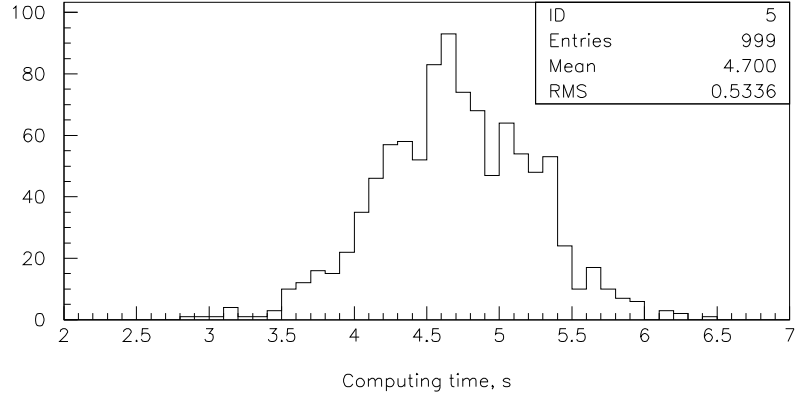


Figure 9: MC test results for $c_y = c_z = 0.002$ rad.

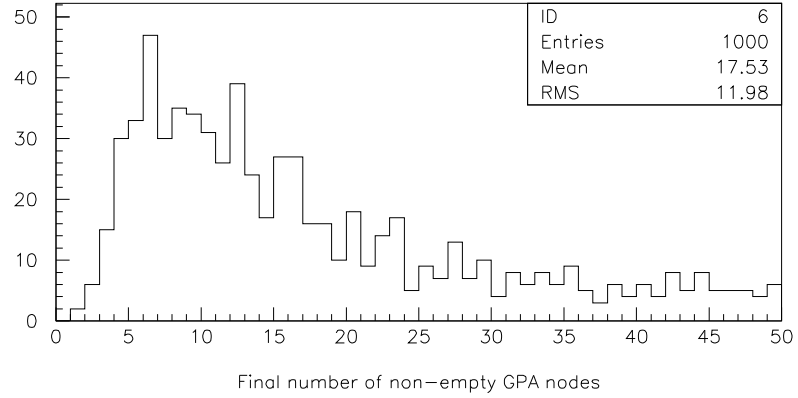
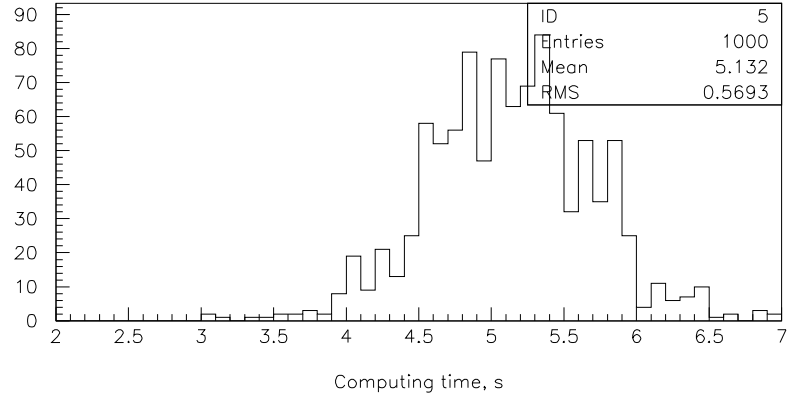


Figure 10: MC test results for $c_y = c_z = 0.003$ rad.

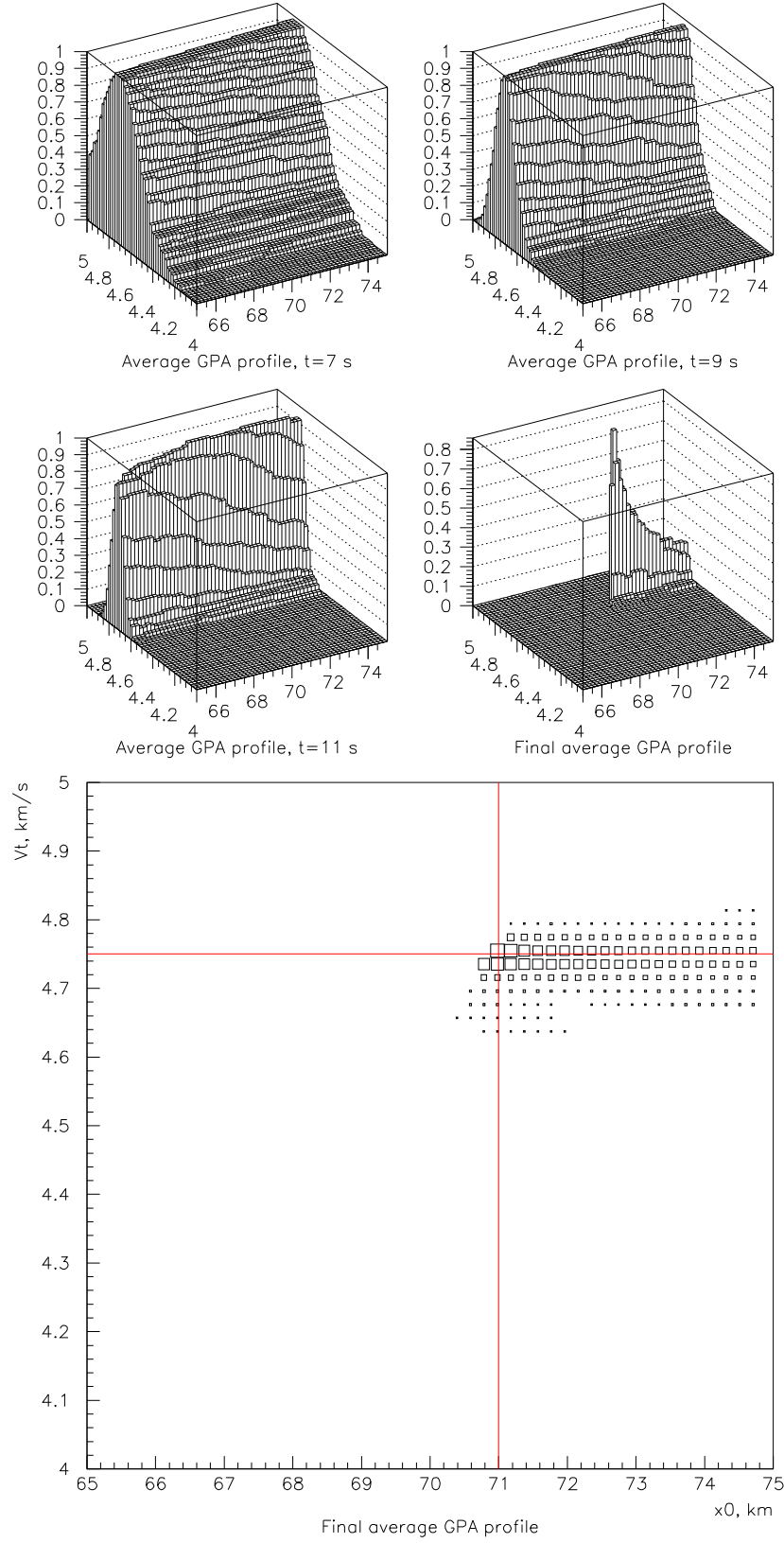


Figure 11: Average GPA profiles for $c_y = c_z = 0.001$ rad.

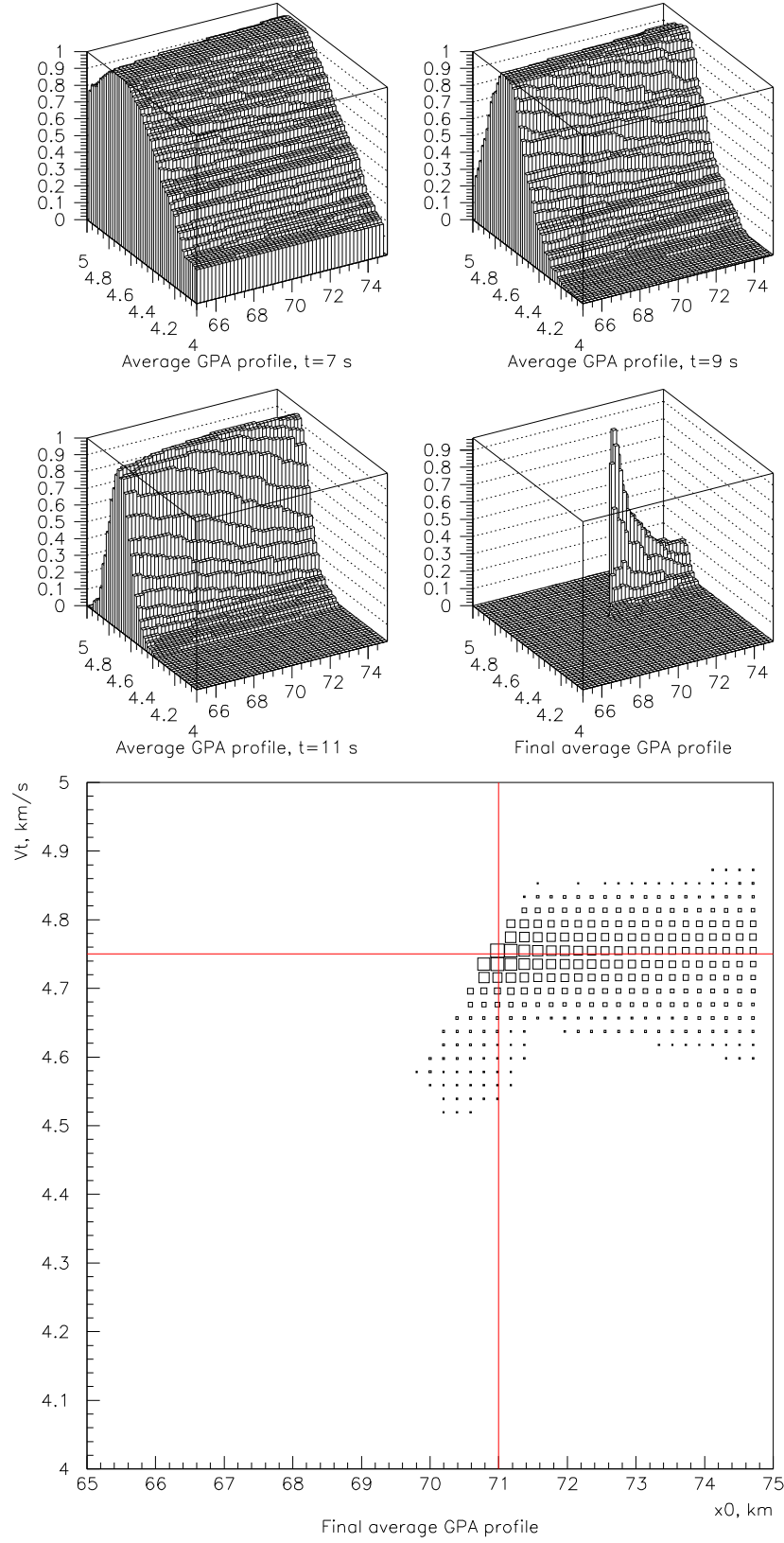


Figure 12: Average GPA profiles for $c_y = c_z = 0.002$ rad.

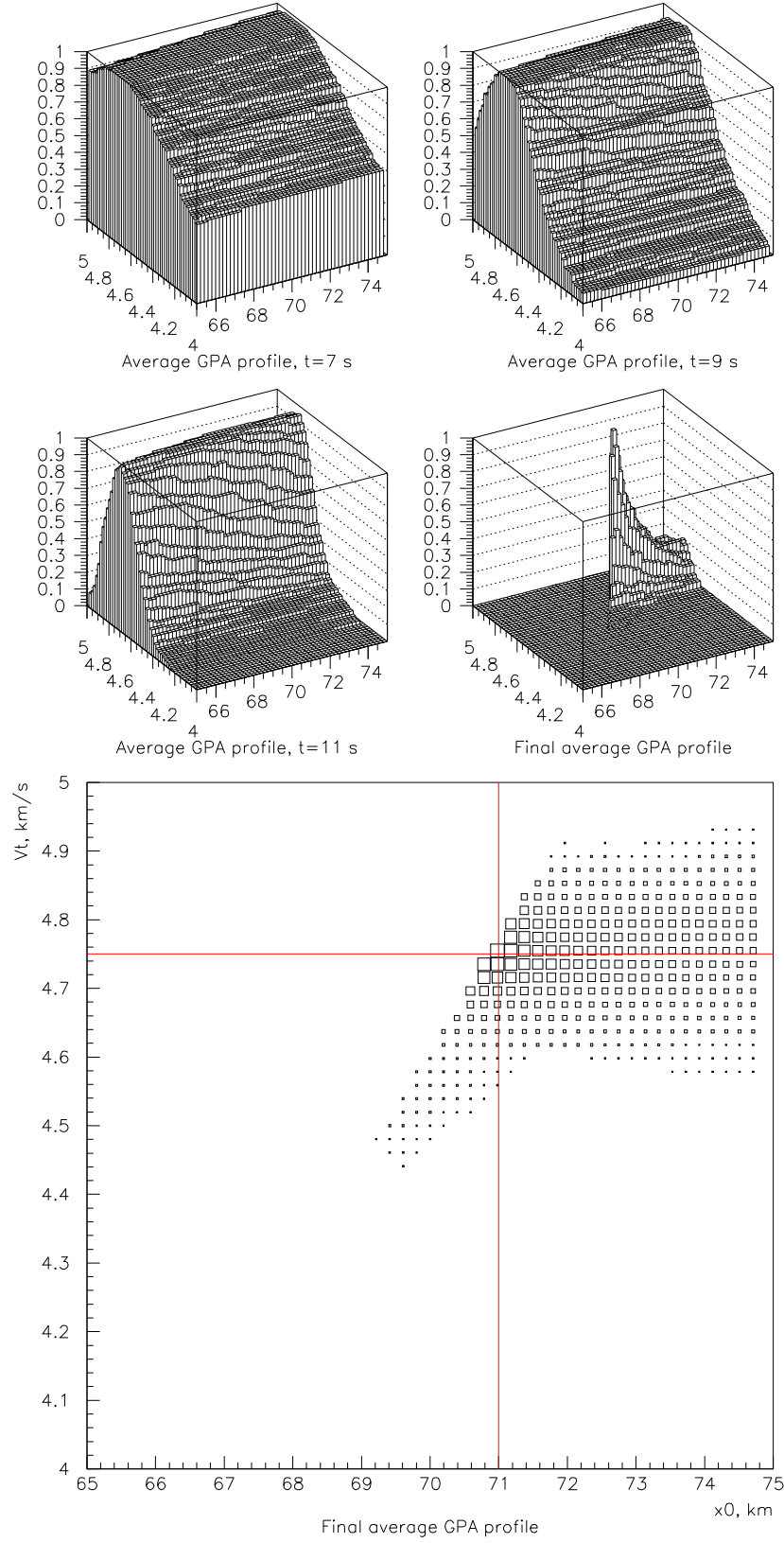


Figure 13: Average GPA profiles for $c_y = c_z = 0.003$ rad.

7.4 Resume

The results obtained during MC test of the proposed guidance algorithm show that

- The algorithm provides precise and unbiased guidance, the distributions of terminal misses are symmetrical without pronounced tails for both, **OY** and **OZ**, control directions.
- The consumption of control impulses during guidance depends on given measurement errors and tends to the optimal solution with complete information when the measurement precision is increased.
- The proposed algorithm is numerically stable, no cases of GPA degeneration have been observed during 3000 MC runs with different values of measurement errors.
- The final average distribution of non-empty GPA nodes has pronounced single peak corresponding to the true values of x_0 V_T target motion parameters. It means that the algorithm can identify these unknown parameters correctly and GPA finally converges to them. The speed of such convergence is higher for more accurate measurements.
- The mean computing time of the algorithm highly depends on the measurement accuracy and decreases when the accuracy is increased. It can be explained by fast convergence of GPA in case of more accurate measurements. In turn, low number of remaining GPA nodes leads to the faster work of the algorithm.

8 Monte Carlo test of the algorithm of guidance to a maneuvering target

In this section we present and discuss results of Monte Carlo tests which have been conducted for the algorithm of guidance to a maneuvering decelerating target.

As we mentioned above, it is assumed that the target can perform evasive maneuvers by changing its sliding and attack angles. In turn, it leads to additional non-zero lateral acceleration which change the direction of the target's velocity vector in chosen coordinate system. In order to describe this mechanism of the target's maneuver in the framework of IS-based approach we assume that lateral acceleration of the target can change instantly remaining within given boundaries.

At the beginning, we confirm by Monte Carlo simulation that the algorithm of guidance to a non-maneuvering target considered above fails in the case when the targets makes an evasive maneuver. As was shown, not taking a maneuver into account causes fast degeneration of GPA's nodes and large terminal misses which allows the target to avoid an intercept.

Then we show that the algorithm proposed in section 6 provides reliable guidance to a maneuvering target. The distributions of terminal misses for this algorithm are significantly better than that for the algorithm of guidance to a non-maneuvering target. Results regarding to expense of controlling impulses are compared with the optimal solution of guidance problem with complete information. Also we consider aspects of the algorithm's computational properties, in particular, required computing time and numerical stability of the algorithm.

8.1 A priori data

The flow chart of the guidance process simulation in the case of maneuvering target is shown in Fig.14. In comparison with the chart in Fig.5, this one has additional blocks "Simulation of target maneuver" and "Linear transformation of GPA nodes".

This algorithm was implemented in C program module and tested on PC Pentium III 500 MHz too.

All the a priori data were the same as in the case of non-maneuvering target. Namely, the GPA consisted of $51 \times 51 = 2551$ nodes:

$$x_i = x_0 + i\Delta_x, \quad V_{Tj} = V_0 + j\Delta_V, \quad i, j = 0, \dots, 50,$$

where

$$x_0 = 65000 \text{ m}, \quad \Delta_x = 200 \text{ m}, \quad V_0 = 4000 \text{ m/s}, \quad \Delta_V = 200 \text{ m/s}$$

The initial GPA polygons have been assumed to be rectangles defined by the fol-

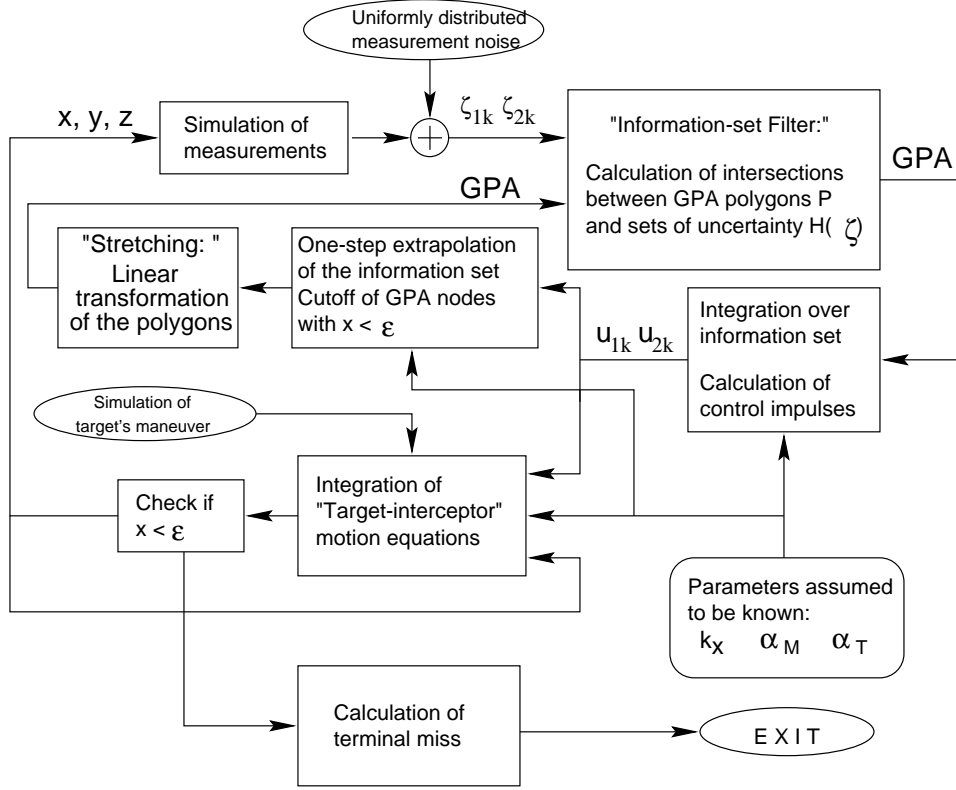


Figure 14: Simulation of the guidance process to a maneuvering target.

lowing inequalities

$$\begin{aligned}
 y_0^* + \delta y \eta_y - \Delta_y &\leq y \leq y_0^* + \delta y \eta_y + \Delta_y, \\
 z_0^* + \delta z \eta_z - \Delta_z &\leq z \leq z_0^* + \delta z \eta_z + \Delta_z, \\
 \sin(\varphi - \Delta_\varphi) &\leq k_y \leq \sin(\varphi + \Delta_\varphi), \\
 \cos(\varphi + \Delta_\varphi) \sin(\varphi - \Delta_\varphi) &\leq k_z \leq \cos(\varphi - \Delta_\varphi) \sin(\varphi + \Delta_\varphi),
 \end{aligned}$$

where y_0^* , z_0^* are initial positions which provide zero terminal miss on free (i.e. with zero controls) motion of the "target-interceptor" system, η_y , η_z – random values uniformly distributed over $[-1, 1]$ interval. The other parameters are the following

$$\begin{aligned}
 \delta y &= 100 \text{ m}, \quad \delta z = 100 \text{ m}, \quad \Delta_y = 3000 \text{ m}, \quad \Delta_z = 3000 \text{ m}, \\
 \Delta_\varphi &= 5.0 \text{ grad}, \quad \Delta_\psi = 5.0 \text{ grad}
 \end{aligned}$$

The algorithm was tested on a model with parameters from Table.1 under three different values of restrictions imposed on measurement errors represented in Table.2.

As was mentioned above, we consider the following mechanism of the target's maneuver. At some instants t_ψ , t_φ , the angles ψ , φ which determine a position of the target's velocity vector start changing (Fig.15). The rates $\dot{\psi}$, $\dot{\varphi}$ are assumed to be constant. The maneuver durations are T_ψ , T_φ for angles ψ , φ correspondingly.

For the Monte Carlo simulation described here, the following values have been taken (Table 4).

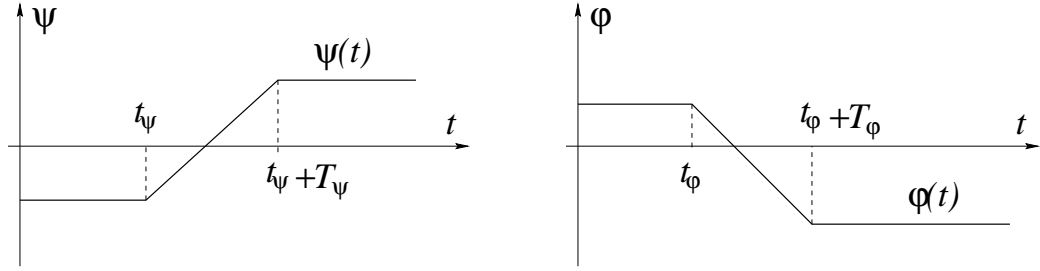


Figure 15: Evolution of ψ and φ during target's maneuver.

Parameter	Value	Parameter	Value
t_ψ	5.0 s	t_φ	5.0 s
T_ψ	0.2 s	T_φ	0.2 s
ψ	0.2 grad/s	φ	0.2 grad/s

Table 4: Maneuver parameters taken for the Monte Carlo simulation.

In order to take possible target's maneuvers into account, the GPA polygons have been subjected to a special linear transformation in addition to the one-step extrapolation of their vertices in accordance with (35). The transformation parameters A_y , A_z have been takes as (Table 5)

Parameter	Value	Parameter	Value
A_y	$3.5 \cdot 10^{-4} \text{ s}^{-1}$	A_z	$3.5 \cdot 10^{-4} \text{ s}^{-1}$

Table 5: Parameters used for transformation of GPA's polygons.

8.2 Evaluation of the guidance algorithm performance

To estimate performance of the guidance algorithm, we have used the same method as in section 7.2, namely, the following values have been calculated after each MC run:

1. Terminal misses along **Y** and **Z** axis M_y , M_z .
2. Consumption of control impulses, R_y and R_z

$$R_y = \sum_{t_k < t_f} |u_{1k}|, \quad R_z = \sum_{t_k < t_f} |u_{2k}|,$$

where t_f is the instant of guidance process termination.

8.3 Computational properties of the algorithm

As in the case of non-maneuvering target, in order to evaluate the computational properties of the proposed algorithm we have investigated

- Possibility of GPA degeneration when it prematurely collapses and there is no non-empty nodes at the end of the guidance.
- Convergence of GPA to the true values of x_0 and V_T parameters. In case of convergence all non-empty nodes of GPA should be located around point corresponding to the true values of x_0 and V_T .
- Computational speed of the algorithm and timing of different parts of the algorithmic procedure.

The correct convergence of the GPA have been checked by investigating so-called average GPA profiles for different instants of time. These two-dimensional distributions are calculated as follows

$$\mathcal{P}_{ij}(t) = \frac{\sum_{k=0}^{N_{runs}} E_k(i, j, t)}{N_{runs}},$$

where N_{runs} – number of MC runs taken for averaging, $E_k(i, j, t)$ equals to 1 if GPA node (i, j) at the moment t is non-empty during MC run number k , and equals to 0 if this node is empty.

8.4 Results of the Monte Carlo simulation

As was mentioned above, we have investigated first the behaviour of the guidance algorithm for non-maneuvering target in the case when a target performs a maneuver. Obtained distributions of terminal misses and average GPA profiles are presented in Fig.16 – 18 for three different values of restrictions imposed on measurement errors (Table 2). The true values of x_0 , V_T parameters are marked by haircrosses.

Histograms for the final number of GPA nodes show that premature collapse of GPA have happened very often for the guidance algorithm under consideration. Observed large terminal misses are explained by complete degeneration of the GPA's nodes due to the target's maneuver which is confirmed by corresponding average GPA profiles.

On the contrary, the algorithm proposed for maneuvering target provides very reliable guidance against a maneuvering target. The distributions of terminal misses and consumption of control impulses are presented in Fig.19 – 20. Filled histograms in these figures show results for the optimal solution of guidance problem with exact information. As was mentioned above, term "exact information" means that the initial parameters of the target's motion are taken from Monte Carlo truth. After that the deterministic problem of optimal control is solved. In this problem, the

performance index is a minimization of control expenses while terminal conditions provide zero terminal miss.

The histograms for the mean computing time and number of non-empty GPA nodes at the end of the guidance are presented in Fig.21 – 23.

One can see that zero bin of the histograms for the final number of GPA nodes is empty. It means that during all 3000 (3x1000) MC runs there were no cases of premature collapse of GPA regardless to the measurement accuracy.

The mean computing time and partial timing are summarized in Table 6.

Values of c_y, c_z , rad	0.001	0.002	0.003
Total mean time, s	10.81	13.35	16.27
Polygons intersections, s	2.88	3.54	4.31
Calculation of control, s	4.42	5.46	6.65
One-step GPA extrapolation, s	3.48	4.32	5.28

Table 6: MC test results on computational speed of the algorithm

The correct convergence of the GPA is illustrated by the average GPA profiles shown in Fig.24 – 26. The true values of x_0, V_T parameters are marked by haircrosses.

8.5 Resume

The results obtained during MC test of the proposed guidance algorithm show that

- The algorithm provides precise and unbiased guidance, the distributions of terminal misses are symmetrical without pronounced tails for both, **OY** and **OZ**, control directions.
- The consumption of control impulses during guidance depends on given measurement errors and tends to the optimal solution with complete information when the measurement precision is increased.
- The proposed algorithm is numerically stable, no cases of GPA degeneration due to the target's maneuver have been observed during 3000 MC runs with different values of measurement errors.
- The final average distribution of non-empty GPA nodes has pronounced single peak corresponding to the true values of x_0, V_T target motion parameters. It means that the algorithm can indentify these unknown parameters correctly and GPA finally converges to them. The speed of such convergence is higher for more accurate measurements.

- The mean computing time of the algorithm highly depends on the measurement accuracy and decreases when the accuracy is increased. It can be explained by fast convergence of GPA in case of more accurate measurements. In turn, low number of remaining GPA nodes leads to the faster work of the algorithm.

9 Conclusion

The three-dimensional problem of guidance with incomplete information has been considered. To solve the problem an approach concerned with a construction of information sets (IS) has been used. In terms of IS the original problem has been reduced to an auxiliary impulse control problem and the guidance algorithms against high-speed non-maneuvering and maneuvering targets has been developed. To facilitate numerical operations with the introduced IS, Grid-Polygon Approximation of the IS has been proposed. To estimate performance of the guidance algorithms, Monte Carlo (MC) simulation has been accomplished. The MC simulation has been demonstrated numerical stability of the algorithms and their potential for real-time data processing.

10 Outlook

In our opinion, the future improvements on the proposed algorithms will be mainly concerned with increasing their computational speed. Such an improvement can be done in the different ways.

First, we can use more efficient numerical approximation of the introduced IS. For example, new nodes can be added to the GPA dynamically in order to keep their total number more or less constant in the course of the guidance. Also it might be better to describe the sections of the IS by not simply polygons but by combinations of straight-line segments and segments of some curves of higher order.

Second, as we mentioned above, the MC tests show that the number of GPA nodes remains quite big during all guidance, slowing the algorithms significantly (one run takes about 7 – 10 sec). In turn, this number highly depends on measurement accuracy and decreases when the accuracy is increased. It is natural, because the higher measurement accuracy is, the better observability the system "target-interceptor" has. Measurement accuracy depends on inner parameters of IR array seeker only and cannot be improved by interceptor's impulse control law. In this connection there is the main problem: to reduce the number of remained GPA nodes under given measurement accuracy. To solve this problem we need to improve observability of the system "target-interceptor".

It is well known that in problems of guidance with nonlinear (bearings/range, bearings-only) measurements, the observability explicitly depends on guidance trajectory. So, there is an idea to try so-called trajectory control over observations

[7], [8] to construct a guidance trajectory of special shape that makes "target-interceptor" system more observable and hence improves quality of TMA solution that is of vital importance in the case of engagement with a maneuvering target. The key element of this idea is to add into the performance index of the optimal impulse control problem the special term that has the effect of making the target's motion more observable. The performance index is taken to be the weighted sum of an integral penalty on the magnitude of the interceptor controls and the trace of the Fisher information matrix (observability Gramian). This performance index should be minimized under terminal conditions requiring that the average terminal miss be equal to zero. The averaged miss is defined as a ratio of the integral of the terminal miss function over the IS and the IS phase volume. In our opinion, this is an interesting problem for future investigations.

References

- [1] A.B. Kurzhanskii (1977). *Control and observation in uncertainty conditions*. Nauka, Moscow.
- [2] F.L. Chernou'sko and A.A. Melikyan (1978). *Game problems of control and searching*. Nauka, Moscow.
- [3] S.I. Kumkov and V.S. Patsko (1995). Optimal strategies in a pursuit problem with incomplete information. *J. Appl. Math. Mech.* **59**, pp. 75-85.
- [4] S.I. Kumkov and V.S. Patsko (1996). A model problem of space vehicle homing. In: *Proceedings of the Seventh International Symposium on Dynamic Games and Applications* (J.A.Filar, Ed.) Vol.1. Dec. 16-18, 1996, Kanagawa, Japan, pp. 547-556.
- [5] D.D. Emel'yanov (1998). Optimal impulse control of an information set in guidance with incomplete information. *Automation and Remote Control.* **59**, No 3, Part 1, Jan. 1998, pp. 28-35.
- [6] D.D. Emel'yanov (1998). Optimization of impulse control in one problem of guidance with incomplete information. *Proceedings of the III IFAC Workshop "Singular Solution and Perturbations in Control Systems"*, Pereslavl-Zalessky, Russia, 7-11 July 1997. Pergamon Press, 1998, pp. 103-107.
- [7] D.D.Emel'yanov (1997). Trajectory Control of Observations. *Automation and Remote Control.* **58**, No 10, Part 1, Oct. 1997, pp. 1592-1601.
- [8] E.Ya.Rubinovich (1980). The path observation control in discrete stochastic problems of optimization. *Automation and Remote Control.* **41**, No 3, Part 1, March 1980, pp. 365-372.

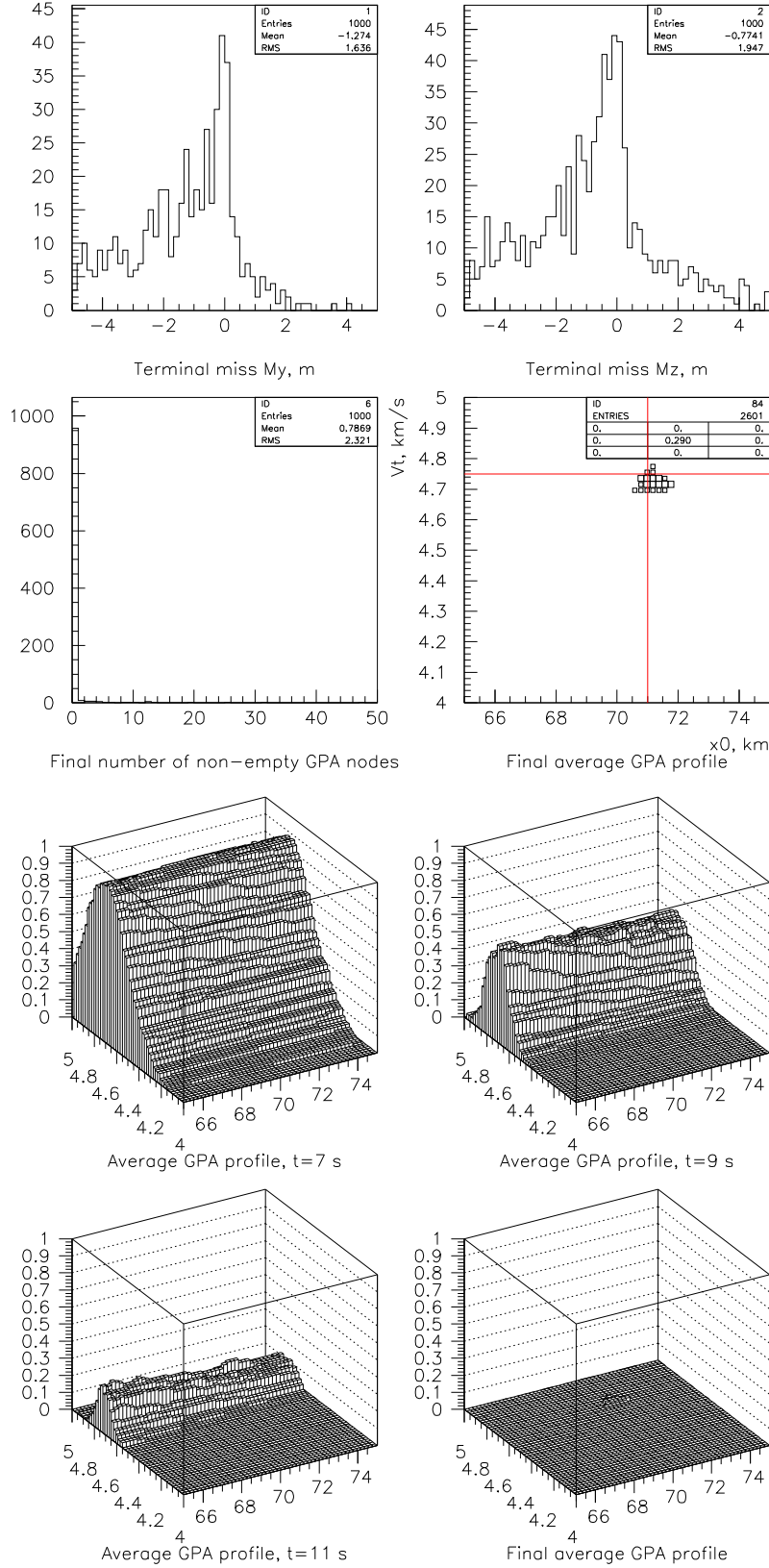


Figure 16: MC test results for $c_y = c_z = 0.001$ rad.

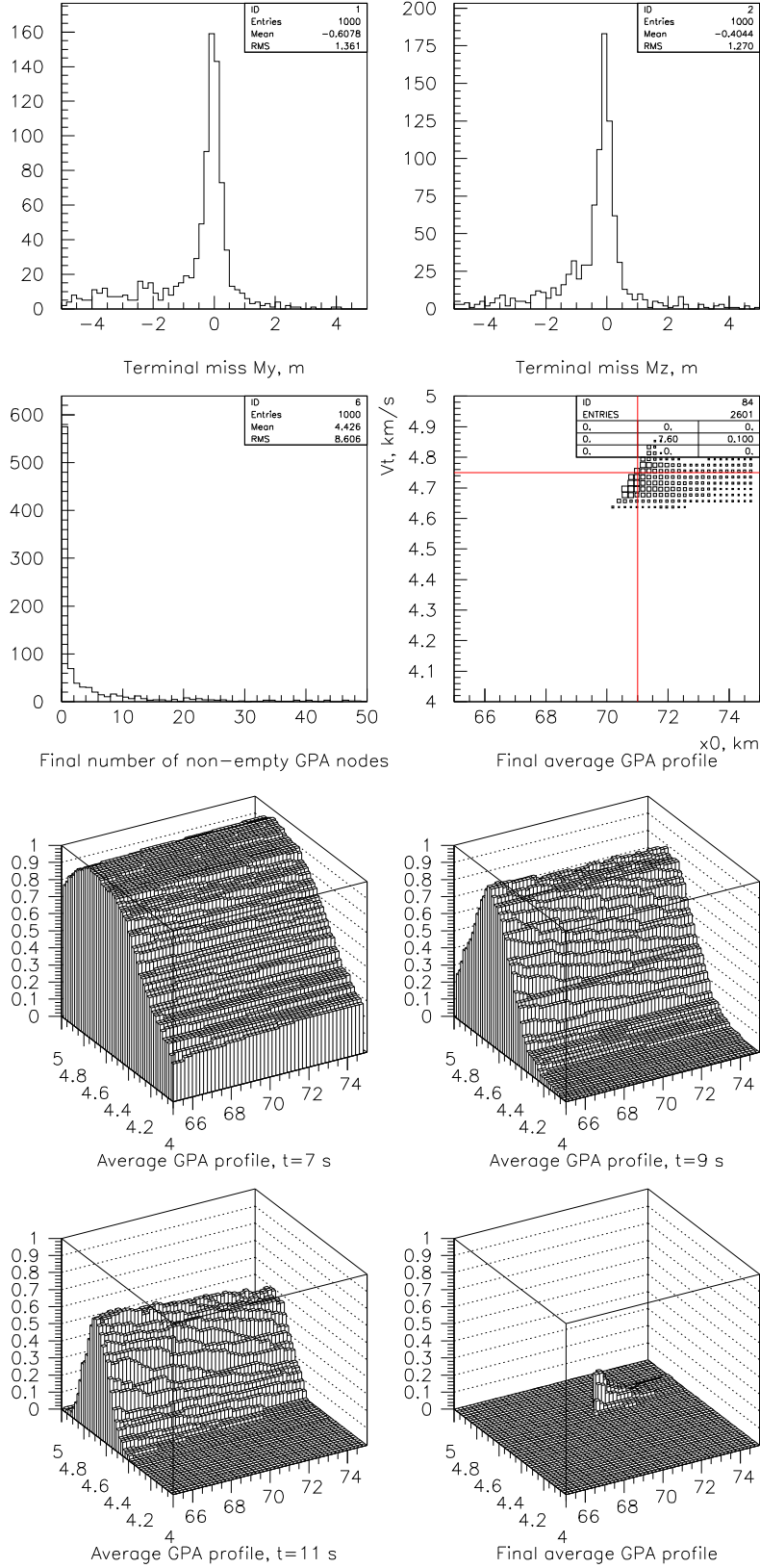


Figure 17: MC test results for $c_y = c_z = 0.002$ rad.

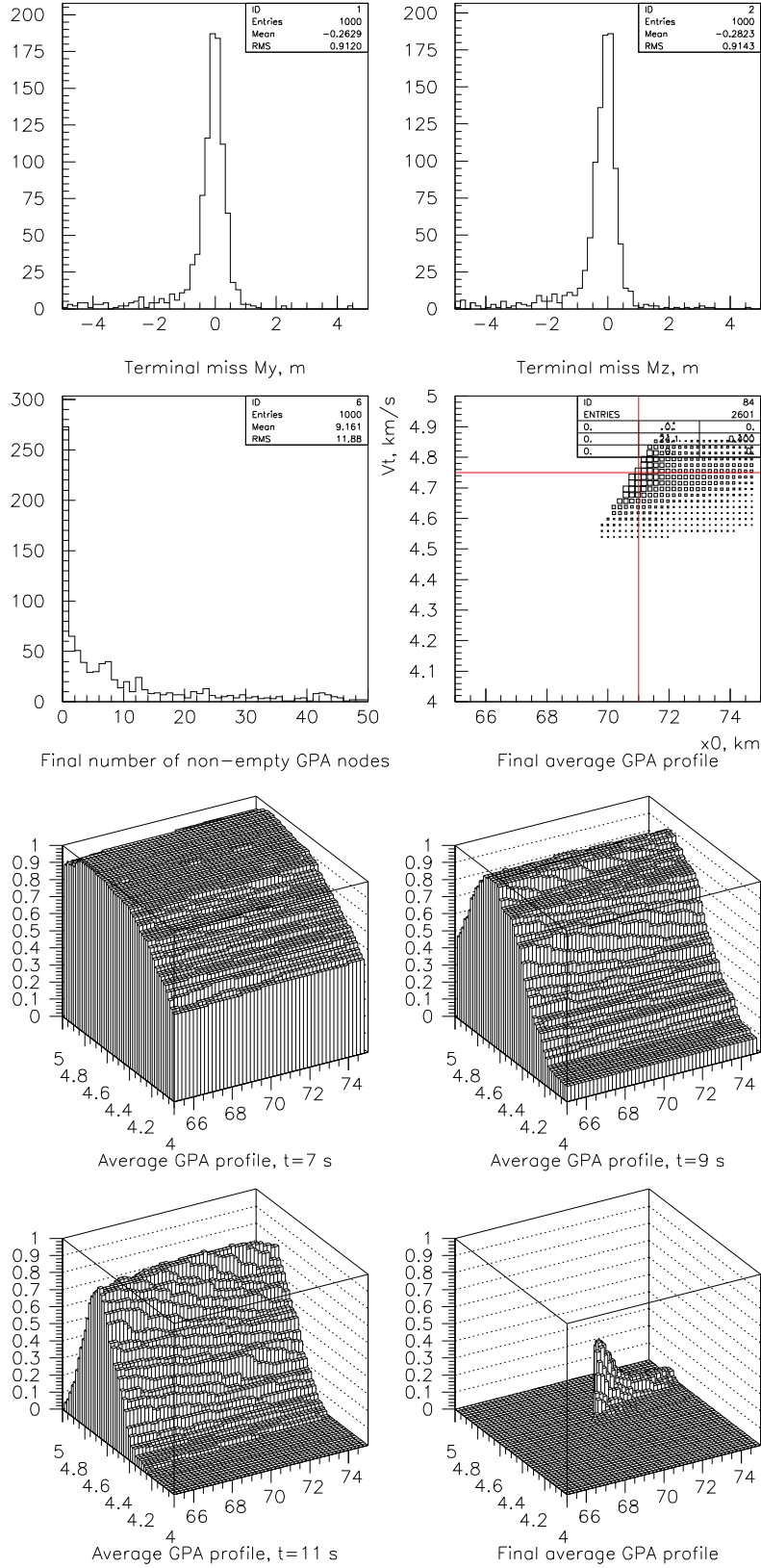


Figure 18: MC test results for $c_y = c_z = 0.003$ rad.

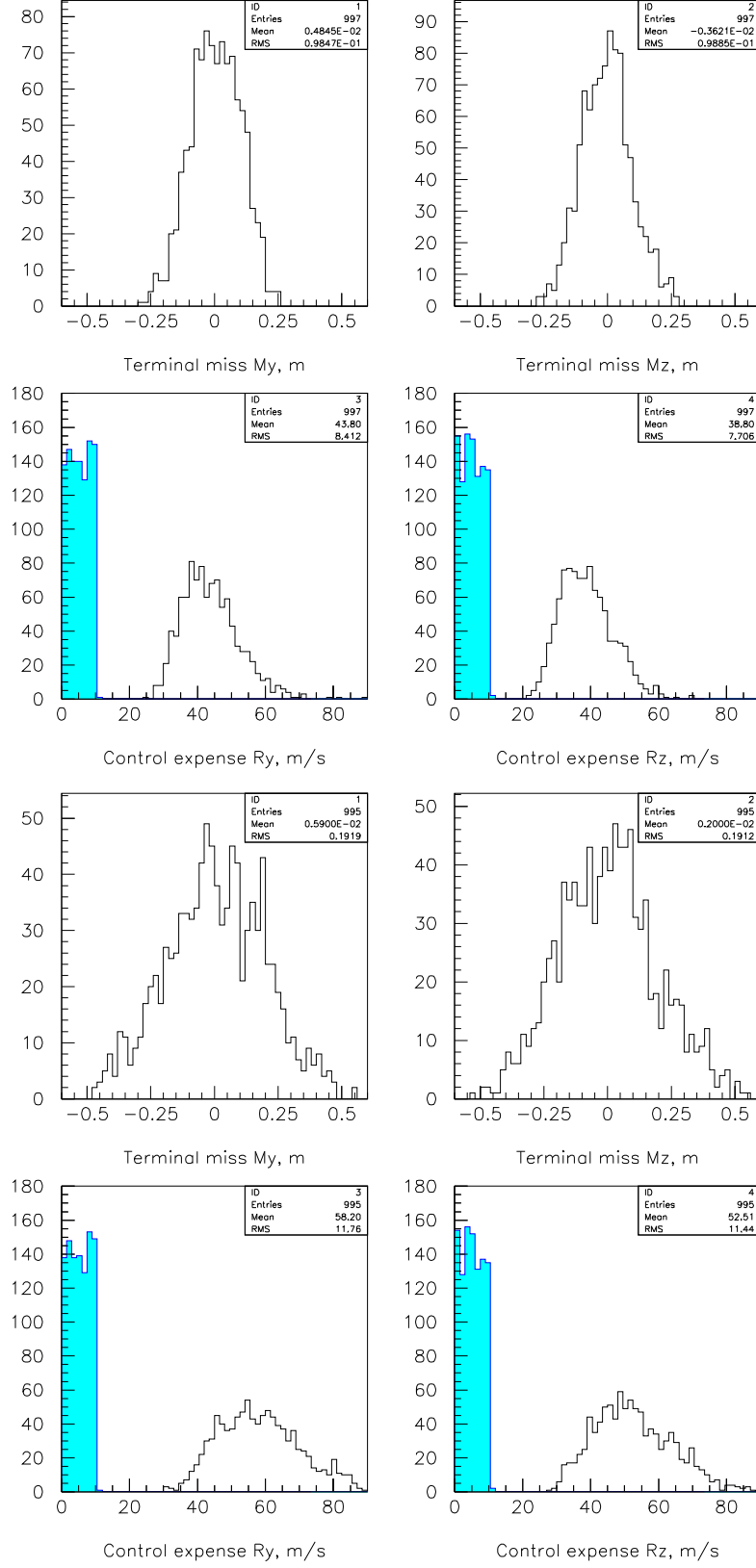


Figure 19: MC test results for $c_y = c_z = 0.001$ rad (two upper plots) and $c_y = c_z = 0.002$ rad.

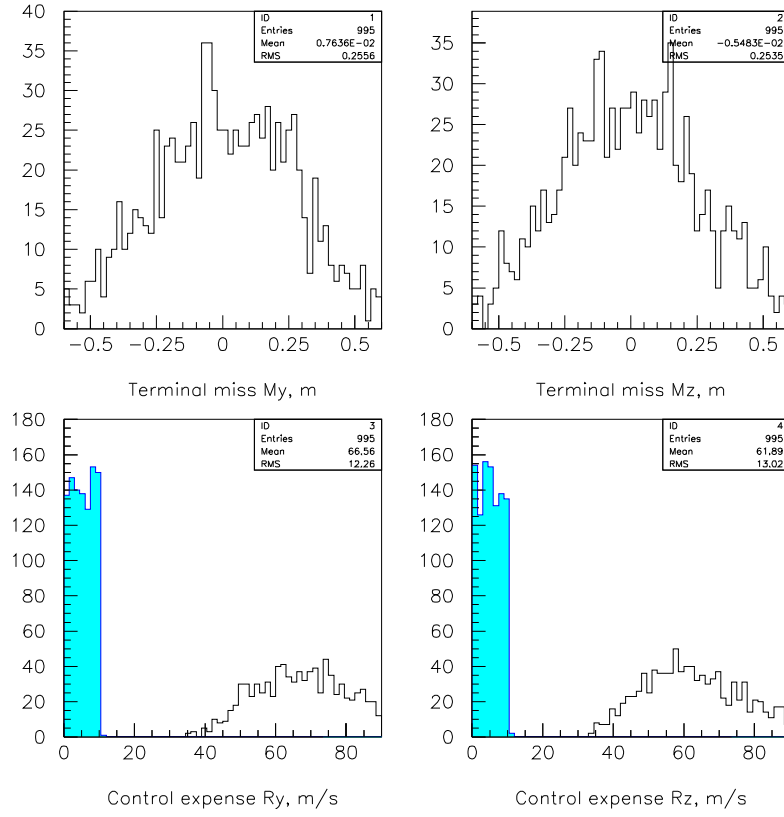


Figure 20: MC test results for $c_y = c_z = 0.003$ rad.

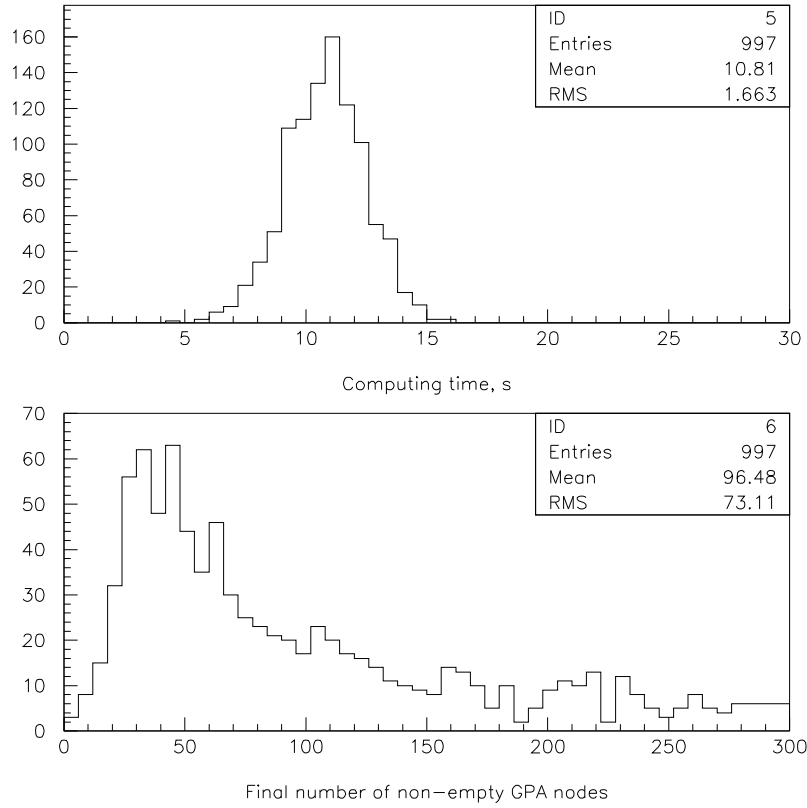


Figure 21: MC test results for $c_y = c_z = 0.001$ rad.

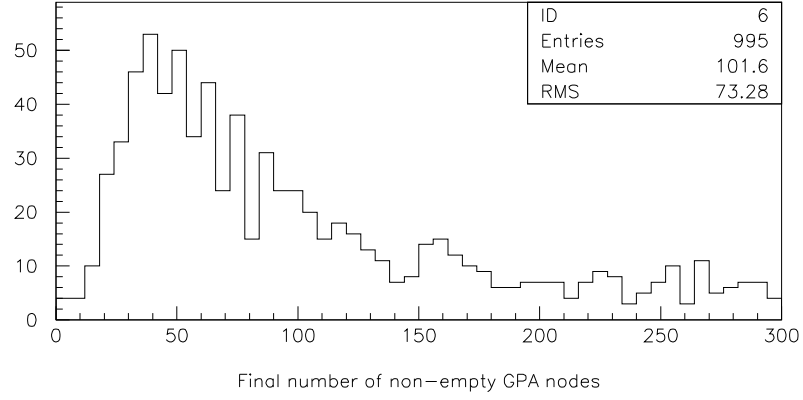
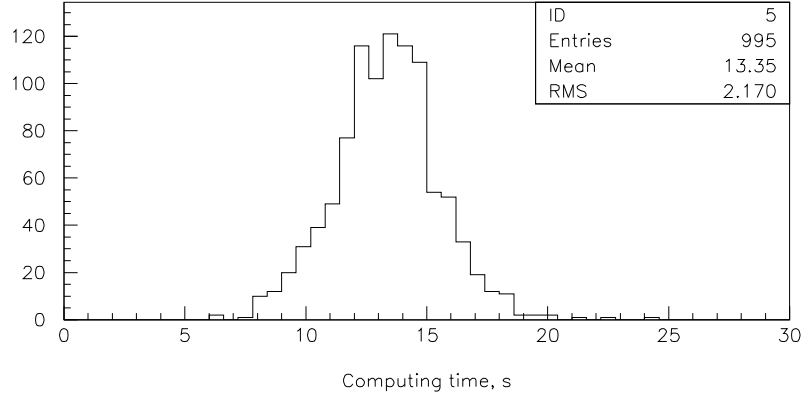


Figure 22: MC test results for $c_y = c_z = 0.002$ rad.

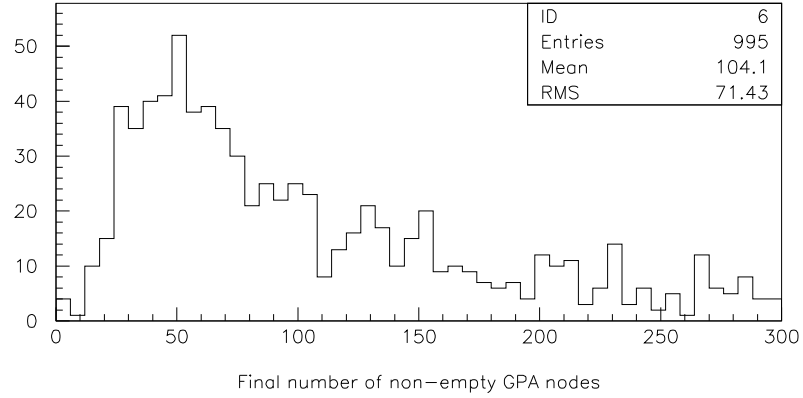
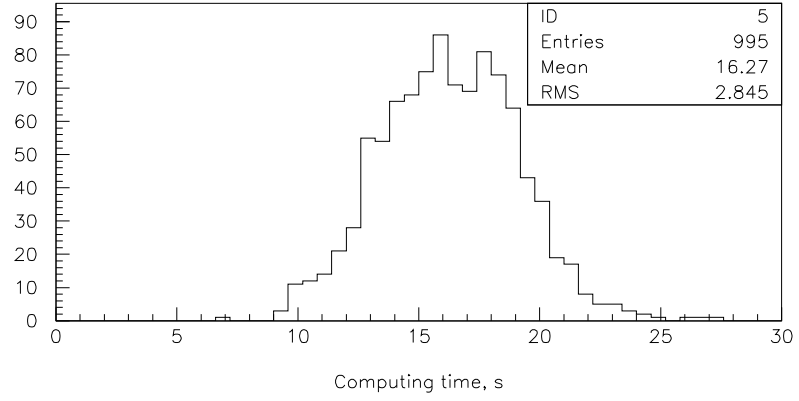


Figure 23: MC test results for $c_y = c_z = 0.003$ rad.

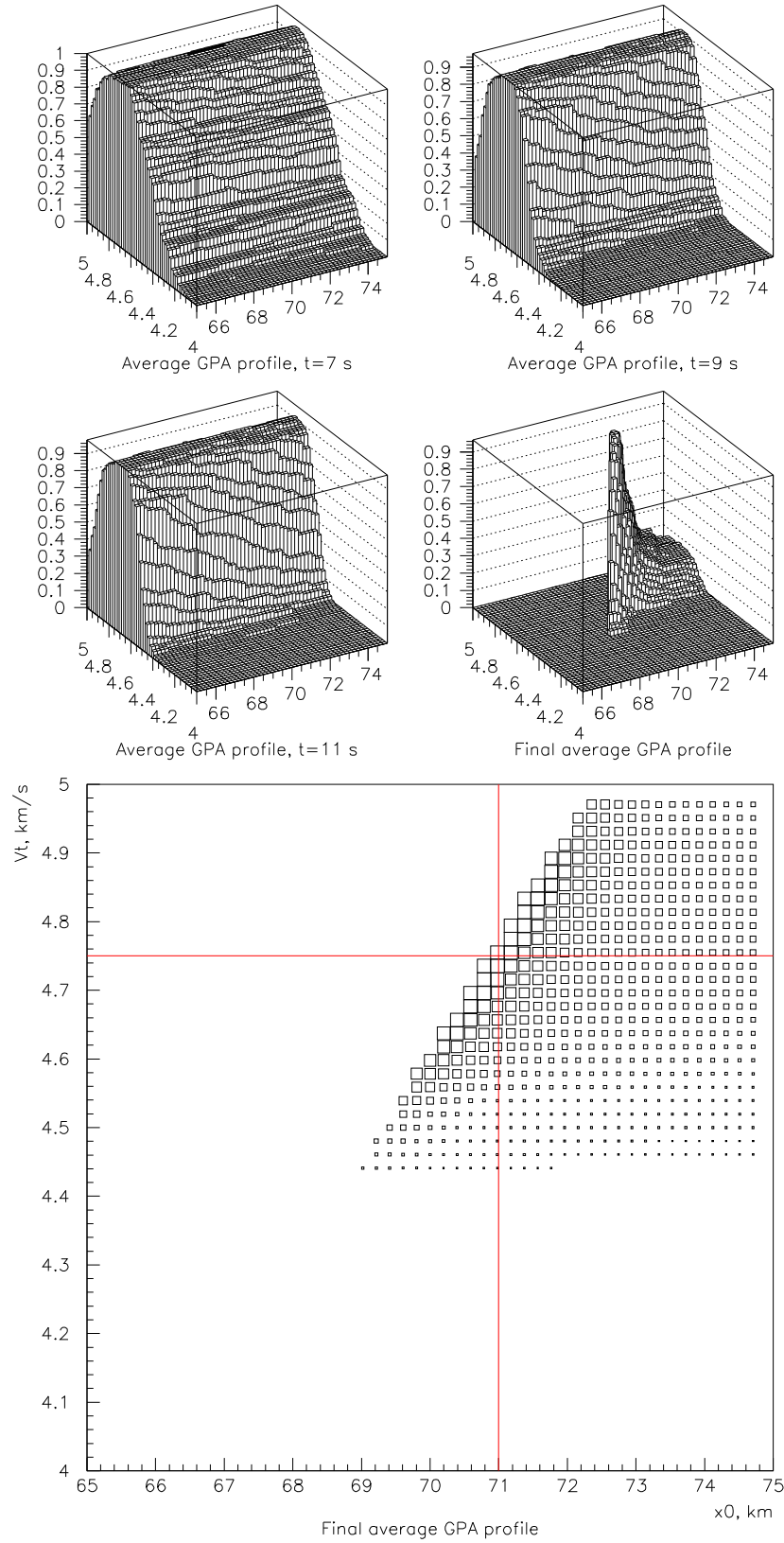


Figure 24: Average GPA profiles for $c_y = c_z = 0.001$ rad.

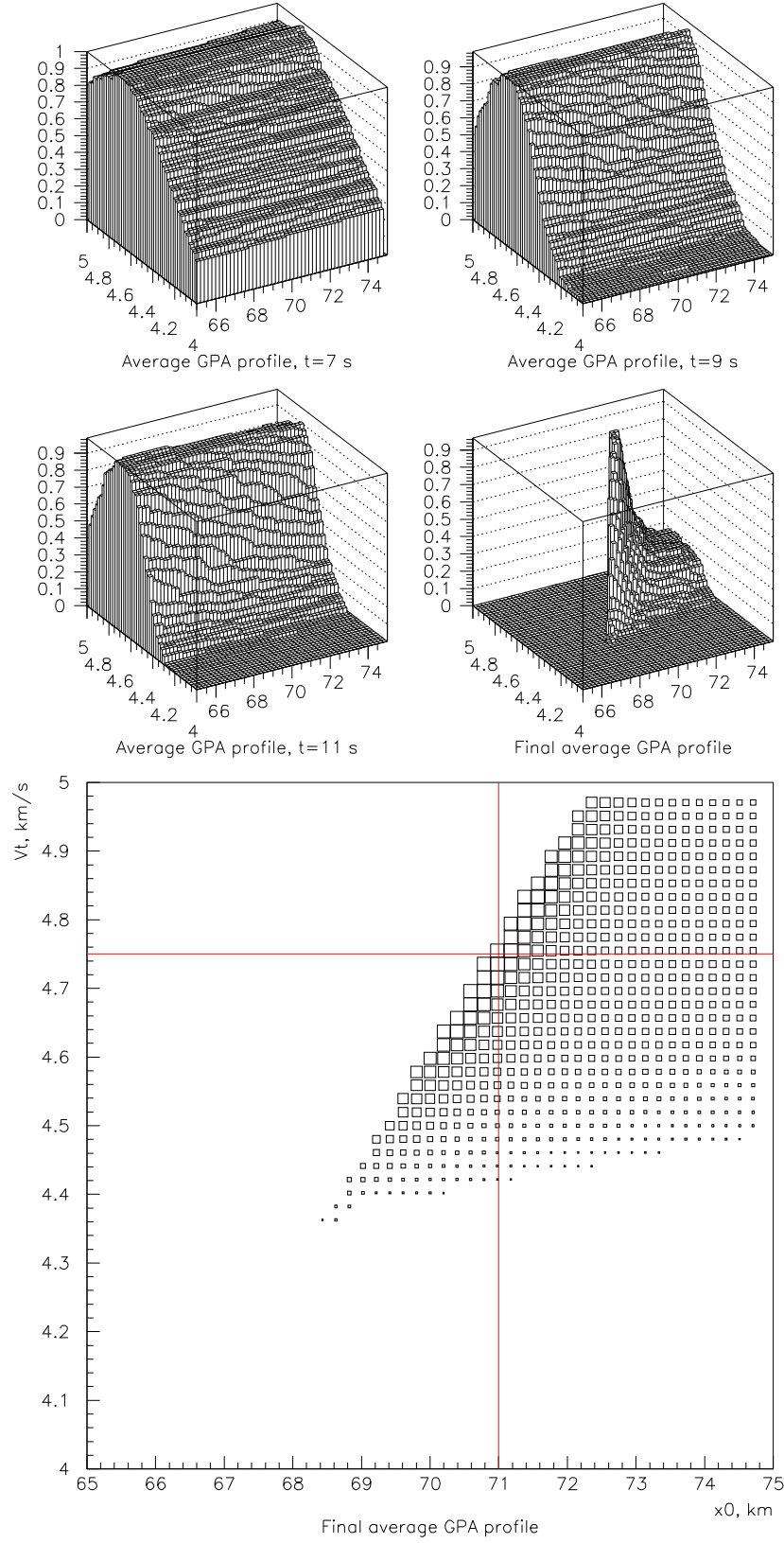


Figure 25: Average GPA profiles for $c_y = c_z = 0.002$ rad.

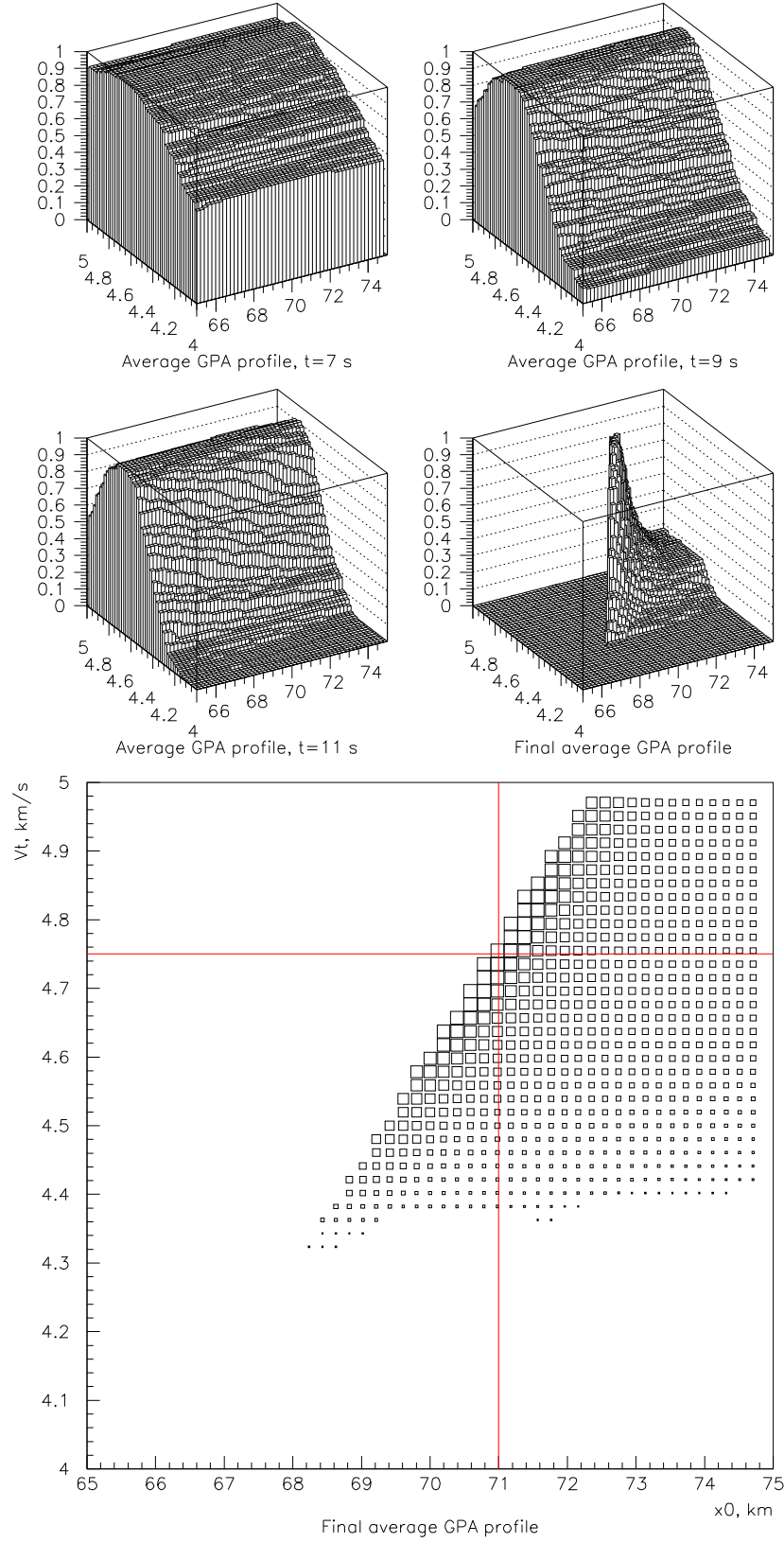


Figure 26: Average GPA profiles for $c_y = c_z = 0.003$ rad.